DOE Final Report

DOE DE-FG0298ER14897

Very High Pressure Single Pulse Shock Tube Studies of Aromatic Species

Prof. Kenneth Brezinsky (PI)

Department of Mechanical & Industrial Engineering,
University of Illinois at Chicago,
2039, Engineering Research Facility, M/C 251,
842, W. Taylor St., Chicago, IL 60607.
Kenbrez@uic.edu

Table of Contents

Table of Figures

Abstract:

The principal focus of this research program is aimed at understanding the oxidation and pyrolysis chemistry of primary aromatic molecules and radicals with the goal of developing a comprehensive kinetic model at conditions that are relevant to practical combustion devices. A very high pressure single pulse shock tube is used to obtain experimental data over a wide pressure range in the high pressure regime, 5-1000 bars, at pre-flame temperatures for fuel pyrolysis and oxidation over a broad spectrum of equivalence ratios. Stable species sampled from the shock tube are analyzed using standard chromatographic techniques using GC/MS-PDD and GC/TCD-FID. Experimental data from the HPST (stable species profiles) and data from other laboratories (if available) are simulated using kinetic models (if available) to develop a comprehensive model that can describe aromatics oxidation and pyrolysis over a wide range of experimental conditions. The shock tube has been heated (100^0C) recently to minimize effects due to condensation of aromatic, polycyclic and other heavy species. Work during this grant period has focused on 7 main areas summarized below.

(a) Toluene Oxidation:

A detailed chemical kinetic model[1] has been developed to predict the oxidation of toluene in the high temperature regime over wide pressure ranges based on experimental data[2] obtained in the high pressure single pulse shock tube at the University of Illinois at Chicago. Toluene oxidation experiments span a temperature range from 1210 -1480 K and pressures from 22-550 bars[2]. Experiments were performed for stoichiometric (Φ=1) and fuel rich (Φ=5) mixtures. The primary stable species observed in the Φ=1 experiments were C_6H_6, C_2H_2, CO, CO_2, C_2H_4 with trace amounts of C_2H_6 and 1,3 C_4H_6. The 550 bar Φ=1 experiments used very dilute initial mole fractions (8 ppm) of the fuel, toluene. For the lower pressure 50 bar and 22 bar experiments, when the heated sample rig was available, higher initial fuel mole fractions of 75 ppm and 72 ppm were used respectively. Since very dilute reagent mixtures (8-85ppm) were used in all the experiments reported in this work the heat release was minimal and through calculations was shown to lead to no more than a 5 K temperature rise exhibited by the more concentrated toluene mixtures (75 ppm used for the 50 bar, Φ=1 set) under the reaction conditions of our study. Thus, the reactions occur under essentially isothermal conditions. The carbon totals for the Φ=1 experiments show no more than a 15% discrepancy at the highest temperatures (1400 K) in the current experiments. In the case of the Φ=5 experiments significant amounts of diacetylene, C_4H_2, were also observed in addition to the species seen in the Φ=1 experiments. Figures 1 and 2 are representative species profiles obtained for Φ=1 experiments at 550 bars and for Φ=5 experiments at 22 bars respectively. The species profiles for the lower pressure data sets (50 and 22 bars) for the Φ=1 experiments exhibit similar qualitative trends with the onset of toluene decay and corresponding buildup of the intermediates and products occurring at progressively higher temperatures as the pressure is reduced. The same qualitatively consistent trends are seen for the Φ=5 experiments. Furthermore at any given pressure the onset of toluene decay occurs at much lower temperatures for the Φ=1 experiments as compared to the Φ=5 experiments. A detailed discussion of the experimental data/results is provided elsewhere[2].

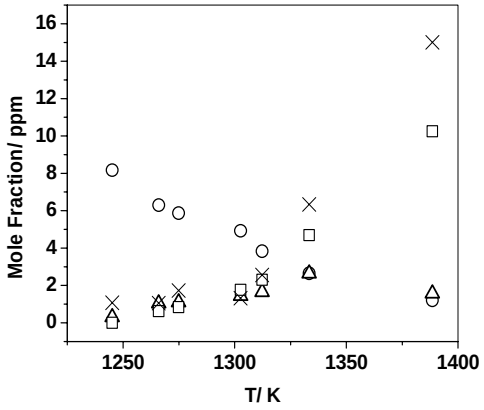

Fig 1: 550 bars, Φ=1. O-$C_6H_5CH_3$, Δ-C_6H_6, □-CO, X- CO_2.

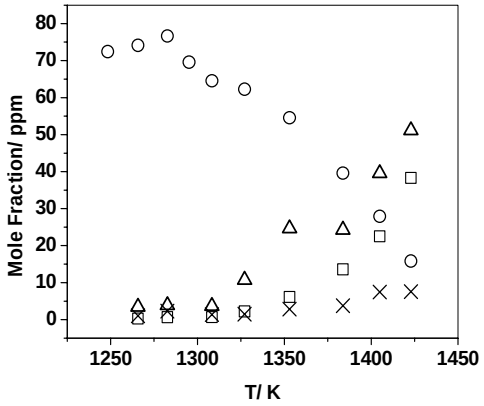

Fig 2: 22 bars, Φ=5. O-$C_6H_5CH_3$, Δ-CO, □-C_2H_2, X- CO_2.

The experimental data represent the first high pressure, high temperature study on the oxidation of toluene. The above data set extends the range of experimental data to encompass as well as exceed pressures encountered in practical combustion systems and serves to test how well current lower pressure models predict the combustion of toluene at elevated pressures and temperatures. Furthermore these lower pressure models can be used as a starting point to develop comprehensive models applicable over very wide pressure and temperature ranges. We have used two of the more recent models, the KBG model[3] and the Dagaut et al.[4] model as a starting point to develop a comprehensive model. Figure 3 depicts the predictions made by these two recent models to the experimental data. The Dagaut et al. model[4] clearly predicts too slow toluene consumption. The KBG model makes fairly good predictions of the experimental toluene concentrations at temperatures below 1260 K, but at the higher temperatures there is a severe mismatch. The KBG model does a relatively better job at predicting the fuel decay as well as intermediates concentrations and hence is a better choice as a starting point to develop a model to simulate the high pressure shock tube data. The predictions of the KBG model for the toluene concentrations for the 50 bar and 25 bar Φ=1 experiments are good at lower temperatures (as expected since the model was developed and validated against experiments at T<1200 K) but show significant differences from the model

predictions at temperatures beyond 1300 K. The intermediates observed in these experiments namely C_6H_6, CO and C_2H_2 are also correspondingly not well predicted by the model at higher temperatures.

Sensitivity analyses were performed to get a better understanding as to why the KBG model shows increasing deviations from the experimental data at higher temperatures. Figure 4 is a plot of the sensitivity spectrum for three Φ=1 experiments at 1350 K with a nominal reaction time of 1.5 ms. Reactions to which the toluene concentration shows large sensitivities have been plotted for experiments at 610 bars, 50 bars and 25 bars. Numbers refer to reactions in the KBG model. Large sensitivities are seen for reaction 498, the reaction between benzyl, C_7H_7, and HO_2 as well as for 458, phenyl, C_6H_5, and O_2 for the 610 bar experiments. The sensitivity results for the lower pressure experiments at 50 and 25 bars exhibit much smaller sensitivities for these two reactions and would not normally have warranted much attention were it not for their importance at high pressure. A change in the rate coefficients for the most sensitive reactions produces a significant effect on the toluene concentrations at the higher pressures but does not have an effect for the lower pressure experiments. Thus it can be concluded that the discrepancy between the model predictions and the experiment for the lower pressures can only be accounted for by reactions not included in the model.

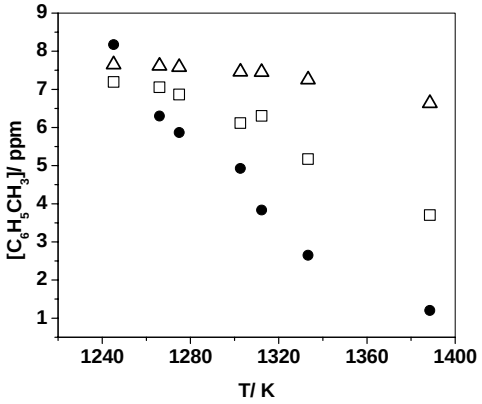

Fig 3: Toluene Oxidation, 550 bars, Φ=1. [●] – Experiment, [Δ] – Dagaut Model, [□] – KBG model.

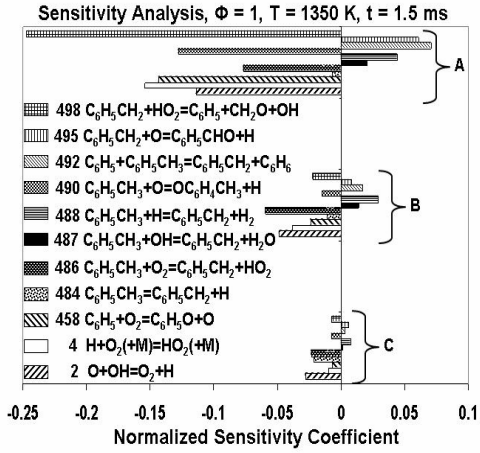

Fig 4: Toluene Oxidation, Sensitivity Spectrum, Φ = 1. [A] – 550 bars, [B] – 50 bars, [C] – 22 bars.

Utilizing the results of the sensitivity analyses and rates of production and comsumption analyses we have updated the rate coefficients for nine of the dominant and sensitive reactions in the KBG model as well as incorporated additional nine high temperature reaction pathways involving the direct rupture of the aromatic ring such as the decomposition of the benzyl radical, phenyl radical and cyclopentadienyl radical which were not present in the original KBG model. The updated reactions and rate coefficients can be obtained elsewhere[1]. With these updated rate coefficients and reactions the modified KBG model is able to simulate the species profiles for the Φ=1 data sets as seen in Figures 5 and 6. The modified model also does an excellent job of predicting higher temperature (1300-1750 K), lower pressure (2-9 atm) ignition delay measurements by Burcat et al.[4] as well as maintaining it predictions to the lower temperature (<1200 K) 1 atm Princeton flow reactor data against which the base KBG model[3] was developed. The new model provides a good fit to all the experimental data for stoichiometric and fuel lean oxidation but provides a less satisfactory fit to the high pressure species profiles for the Φ=5 (fuel-rich) data set. Sensitivity analyses for the fuel rich data indicate that the primary pyrolytic fission steps in toluene via $C_6H_5CH_3=C_6H_5CH_2+H$ (R1) and $C_6H_5CH_3=C_6H_5+CH_3$ (R2) as well as the decomposition

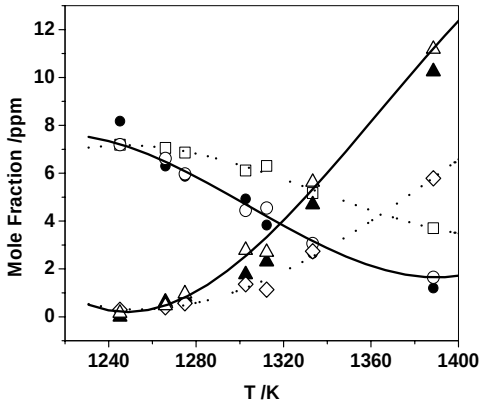

Fig 5: Toluene Oxidation Φ=1, 550 bars. [●] – Expt. $C_6H_5CH_3$, [▲] – Expt. CO, [□] – KBG Model $C_6H_5CH_3$, [◊] – KBG model CO, [o] – Modified Model $C_6H_5CH_3$, [Δ] – Modified Model CO, […] – Fit to KBG Model Predictions, [—] – Fit to Modified Model Predictions.

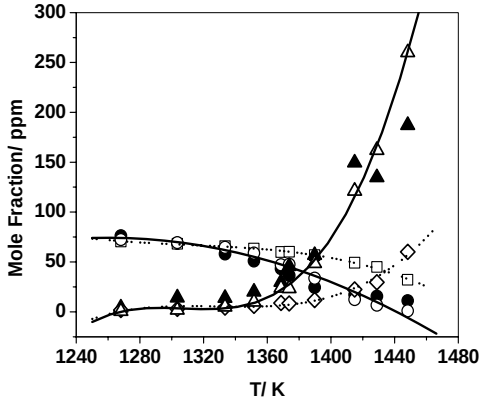

Fig 6: Toluene Oxidation Φ=1, 50 bars. [●] – Expt. $C_6H_5CH_3$, [▲] – Expt. CO, [□] – KBG Model $C_6H_5CH_3$, [◊] – KBG model CO, [o] – Modified Model $C_6H_5CH_3$, [Δ] – Modified Model CO, […] – Fit to KBG Model Predictions, [—] – Fit to Modified Model Predictions.

of the benzyl radical play a key role in the fuel decay process. The current lack of consensus on the primary high pressure limiting branching ratios between R1 and R2 as well as the lack of a validated mechanistic pathway with associated rate coefficients for benzyl decomposition inhibit a better description of the fuel-rich oxidation of toluene. The good agreement between the experimental data that span a wide pressure and temperature range for stoichiometric and fuel lean oxidation and the proposed model indicates that the primary oxidation routes and their rates are validated and forms an important step towards the development of a comprehensive toluene combustion model.

(b) Benzene Pyrolysis:

Despite its limited presence in fuels, benzene is one of the primary intermediates that form during the combustion of higher aromatics. Furthermore it is well known that the high temperature chemistry of benzene plays a significant role in the formation of larger PAH molecules and eventually soot. More recent efforts have also used benzene as a precursor in flames to form fullerenes and high temperature catalytic pyrolysis of benzene to form carbon nanofibers. In spite of its known relevance and utility in a variety of typical combustion devices and processes that operate at high pressures (10-60 atm) the majority of earlier studies were performed under conventional low pressure conditions either using atmospheric pressure reactors or shock tubes at 2-4 atm. Consequently the present study[6] has been performed at higher pressures, 30 - 50 bars, relevant to the operating pressures of practical combustion devices and in the high temperature regime.

Three sets of experiments with more than 60 experiments in total were performed at two sets of nominal reaction pressures, 30 bars and 50 bars over the temperature range 1200 – 1800 K. The reaction times for the experiments were in the range 1.2-1.5 ms. Two sets of experiments were performed at 45 and 50 bars utilizing two reagent mixtures, one with a dilute initial benzene mole fraction of 84 ppm and the other with 800 ppm. The use of the two reagent mixtures provided a test for the reaction order. The third data set at 30 bars was obtained using mixtures with benzene mole fractions of 65 ppm. The primary products detected and analyzed other than benzene were acetylene and diacetylene with acetylene present in copious amounts. Trace amounts of C_2H_4, CH_4, C_2H_6 and C_8H_6 (phenylacetylene) were detected in these experiments but since no more than a few ppm (1-2 ppm) were formed these species were not included in the species plots. Figures 7 and

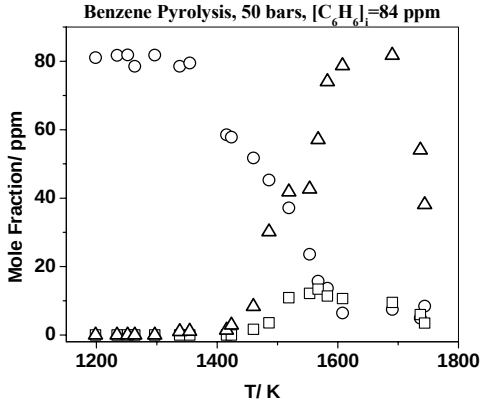

Fig 7: Benzene Data $[C_6H_6]_i$ = 84ppm, O-C_6H_6, Δ-C_2H_2, □- C_4H_2.

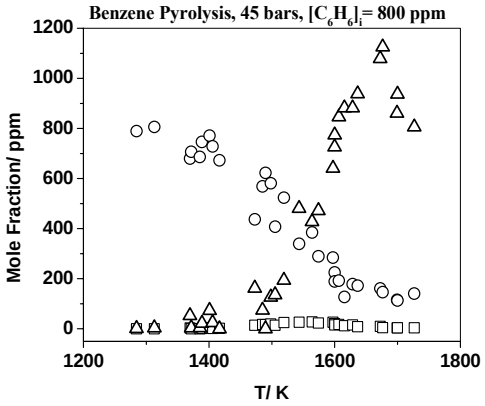

Fig 8: Benzene Data $[C_6H_6]_i$ = 800ppm, O-C_6H_6, Δ-C_2H_2, □-C_4H_2.

8 depict representative species profiles from the 45 bar, 84 ppm and 50 bar, 800 ppm experiments respectively. Benzene starts to decay at temperatures beyond 1400 K and correspondingly the products C_2H_2 and C_4H_2 start to accumulate with copious amounts of acetylene produced at T>1500 K. The carbon totals for the experiments show significant loss of material with upto 50% deviations at the higher extremes of temperature. Significant amounts of soot and PAH are known to be produced under the present high temperature experimental conditions. The experiments were performed in an unheated tube and the heavy molecules most likely condensed on the surface of the shock tube. Furthermore because of the low mole fractions used in this study, the PAHs formed are most likely below the detectable limit. The use of dilute initial mole fractions of benzene results in minimal temperature drop with no more than a 10K drop in temperature due to the endothermicity for the more concentrated 800 ppm experiments at the highest reaction temperatures at the corresponding reaction times for those experiments.

The experimental data has been used to obtain total rates for the decay of benzene over the temperature range 1280-1620 K using a first order Arrhenius expression as shown below where x represents the conversion of the reactant, t the reaction time and

$$k_{Total} = \frac{\ln(1-x)}{t} = A\exp\left(\frac{-E_a}{RT}\right),\ x = \frac{[C_6H_6]_i - [C_6H_6]_f}{[C_6H_6]_i}$$

k_{Total} the overall first order decay rates. Figure 9 represents the benzene total decay rates extracted from the three data sets. The rate parameters obtained from our current high pressure study has been compared against previously reported experimental measurements of overall first order decay rates in Figure 10. Surprisingly for a prototype aromatic such as benzene a large scatter can be observed in earlier reported measurements. At the lower temperature range of our present study (1300 K) there is as much as three orders of magnitude deviation in earlier reported measurements with the deviations reducing at higher temperatures. The current rate is an order of magnitude faster than the flow reactor measurement of Hou and Palmer[7] in the temperature range of overlap (1200 -1500 K) and more than an order of magnitude larger than the Laskin and Lifshitz[8] single pulse shock tube measurements. Extrapolation of the lower temperature (873 -973 K) flow reactor measurement of Banerjee et al.[9] provides a much closer fit to our current study at temperatures up to 1450 K with the flow reactor rate dropping to

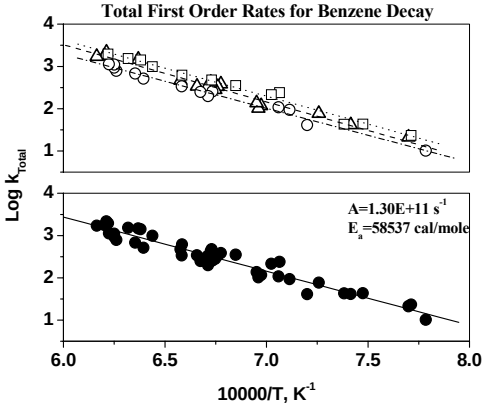

Fig 9: Benzene Decay Rates, O-800 ppm 45 bars, Δ-65 ppm 22 bars, □-84 ppm 50 bars. Dashed lines represent linear fits for the three data sets. ● – First order benzene decay rates for the three data sets. ─ Linear least squares fit to the data.

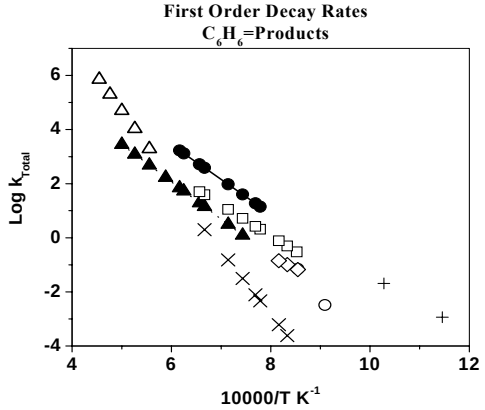

Fig 10: Comparison of literature rates and rates from present work, ● – Present work, ▲-Laskin and Lifshitz[8], O and ◊ - Bruinsma and Geertsman, Δ – Kern et al., □ – Hou and Palmer[7], + - Banerjee et al.[9], X – Baulch et al..

much lower values at higher temperatures.

The experimental results presented in the earlier section represent the first such measurements of species profiles for benzene pyrolysis experiments under conditions of high pressure and high temperature relevant to practical combustion. The data has been used to test current existing mechanisms and models that have been developed for the pyrolysis of benzene. The most recent mechanisms that were developed specifically to describe the high temperature dissociation of benzene are the Laskin and Lifshitz[8] (LL) model and the Wang et al.[10] model. The primary difference in these two models is in the description of the decay of the phenyl radical which governs the formation of the two primary products C_2H_2 and C_4H_2. The two models were assembled in the format required by CHEMKIN and the necessary thermochemical information in the required CHEMKIN format was constructed using the Burcat database[11] and for specific species such as o-C_6H_4 using the heats of formation, entropies and molecular parameters provided in the respective publications.

The predictions made by both the models for the decay of benzene are shown in Figure 11 for the $[C_6H_6]_i$=84 ppm, 50 bar experiments as an example. Both models predict benzene decay to occur at higher temperatures than observed experimentally.

Correspondingly the profile for the major product C_2H_2 is under predicted. The models however are able to make reasonable predictions of the experimental C_4H_2 at lower temperatures below 1600 K. Similar trends are seen for the other two data sets with both the mechanisms severely underpredicting the benzene decay and acetylene formation. The Wang et al.[10] scheme represents the latest benzene mechanism wherein the earlier accepted pathway for phenyl decomposition through the linear C_6H_5 species, the adopted pathway by Laskin and Lifshitz[8] was shown to have no effect. Wang et al.[10] showed that phenyl decay through formation of o-C_6H_4 and subsequent decomposition of the ortho-benzyne was sufficient to model the primary products C_2H_2 and C_4H_2.

Clearly it is seen that in Figure 11 neither benzene model is able to make reasonable predictions of the high pressure data sets obtained in this work. We have therefore chosen a model recently developed in our laboratory[1] as the basis for further development and improvement. The model (Sivaramakrishnan et al.[1]) includes the decay

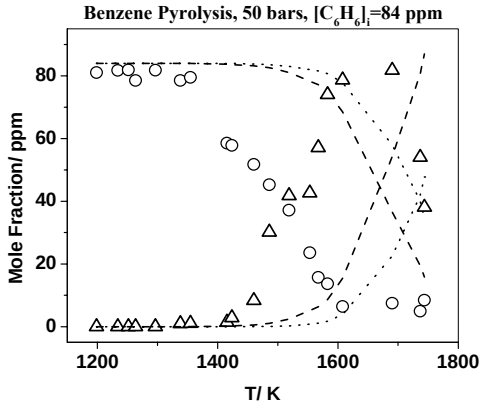

Fig 11: Modeling O - Expt. C_6H_6, Δ – Expt. C_2H_2, ··· - Wang et al.[10] Model, --- - Laskin and Lifshitz[8] model.

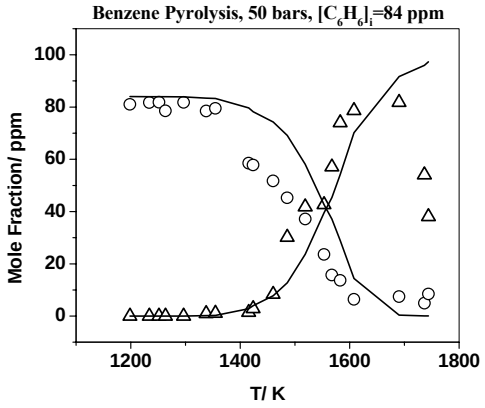

Fig 12: Modeling O - Expt. C_6H_6, Δ – Expt. C_2H_2, — – Current model predictions.

of phenyl by the overall step $C_6H_5 = C_4H_3 + C_2H_2$. A series of steps that describe the phenyl decay better as well as reactions involving the formation of biphenyl were added. Furthermore the rates for the first two steps in the benzene decomposition via $C_6H_6=C_6H_5+H$ and $C_6H_6+H=C_6H_5+H_2$ were updated in the model. The changes and additions made to the Sivaramakrishnan et al.[1] model are outlined in greater detail

elsewhere[6]. The current modified version of the model makes largely improved predictions of the benzene decay and C_2H_2 buildup as shown in Figure 12 for a representative 50 bar, 800 ppm experiments but significantly overpredicts the formation of C_4H_2 (not shown in the Figure 12). Similar predictions were observed for the other two data sets. The current model does not include steps for all the high temperature decay routes of C_4H_2. It has only two principal channels for the decay of diacetylene which are $C_4H_2 + C_2H \rightarrow C_6H_2 + H$ and $C_4H_2 + CH_2 \rightarrow C_5H_3 + H$. However recent studies on C_4H_2 combustion by Hidaka et al.[12] indicate a more complicated scheme for the decay kinetics. Due to the lack of accurate thermochemistry, limited direct kinetic studies and lack of validated rate parameters at high pressures we have at present not included chemical reactions from the Hidaka et al.[12] model to describe the high temperature decay of C_4H_2. We have currently initiated studies into the pyrolysis of diacetylene at high pressures to validate the mechanistic pathways and their associated rate coefficients.

(c) Toluene Pyrolysis:

Prior fuel rich toluene oxidation studies at high pressures in our laboratory[1] have highlighted the dominant role of the pyrolytic channels in toluene decomposition. Furthermore there appears to be a lack of consensus with regard to the branching ratios for the primary fission steps in toluene pyrolysis via channels 1A and 1B below.

$C_6H_5 + CH_3 \rightarrow C_6H_5CH_3$ (1a)

$C_6H_5CH_3 \rightarrow C_6H_5 + CH_3$ (-1a) } Channel 1A

$C_6H_5CH_2 + H \rightarrow C_6H_5CH_3$ (1b)

$C_6H_5CH_3 \rightarrow C_6H_5CH_2 + H$ (-1b) } Channel 1B

Kern et al.[13] have concluded that both the primary channels 1A and 1B are equally dominant at T as low as 1400 K by modeling all the available high temperature data to date in contrast to prior recommendations[14-16] that preferred 1B as the primary dissociation channel. Consequently in order to better characterize the branching ratios and rate coefficients for these channels at high pressures the pyrolysis of toluene has been studied behind reflected shock waves using the UIC single pulse shock tube. Part 1[17] in this two part work focused on the high pressure experimental results and the high pressure limiting rate coefficients for the primary steps in toluene decomposition. Toluene pyrolysis experiments were performed over a wide temperature range from 1200-1900 K at two nominal pressures of 27 and 45 bars with reaction times in the range 1.5 ± 0.2 ms. Experiments were performed using dilute toluene mixtures with mole fractions of 104 ppm that translate to initial concentrations that range from 1.8×10^{-8}-4.9×10^{-8} mol/cc. The low mole fractions minimize temperature drop due to endothermicity, less than 5 K, thereby maintaining essentially isothermal conditions over the time range (1.3-1.7 ms) of the current experiments. A number of intermediates were observed in these experiments principal among these being the smaller hydrocarbons C_6H_6 (Benzene), C_2H_2, CH_4, C_4H_2 (diacetylene), C_4H_4 (vinylacetylene) 1,3-C_4H_6 (1, 3-butadiene), C_2H_6, allene, propyne and the small aromatics phenylacetylene, styrene, p-xylene, ethylbenzene and indene. The carbon totals in these experiments were poor at the higher temperatures beyond 1600 K with carbon recoveries being close to 50%. Formation of small amounts of single ring aromatics and the smallest 5-6 member ring

PAH, indene, in the present experiments offer ample evidence of the presence of heavier aromatics and polycyclics in small amounts that could be condensed on the walls of the shock tube. Furthermore it is well known that acetylene and diacetylene formation lead to subsequent larger polyacetylenes (C_6H_2, C_8H_2) which might explain the poor carbon balance. Representative species profiles for the 45 bar data is shown in Figure 13. Figure 14 shows the overall decay rate coefficients obtained for the decay of toluene using first order kinetics (Equation 1 above) for the 27 and 45 bar experiments. The derived rate coefficients from the present compare favorably against prior measurements. Figure 15 shows the comparison of the total decay rate coefficients obtained in the present work to the prior high temperature measurements and recommendations. The present rate

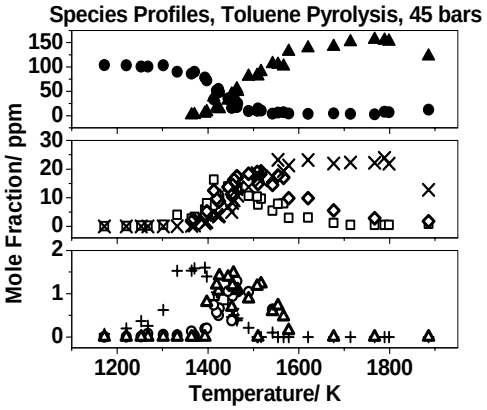

Fig 13: Data [●] – $C_6H_5CH_3$, [□] - C_6H_6, [▲] – C_2H_2, [◊] – CH_4, [X] – C_4H_2, [+] – C_8H_{10} [o] – C_8H_6, [Δ] – C_9H_8.

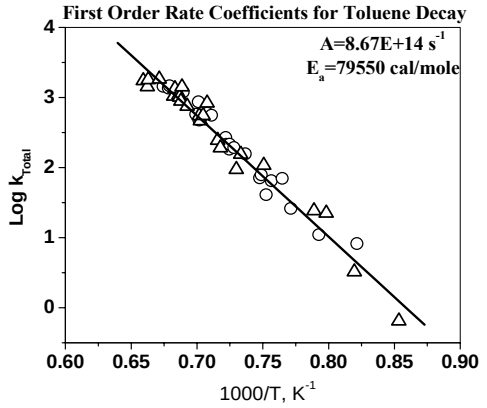

Fig 14: First Order Total Decay Rate Coefficients. [o] –27 bar decay rate coefficients, [Δ] – 45 bar decay rate coefficients, [–] – 27 and 45 bar combined linear fit.

coefficients compare favorably (being less than a factor of two) against those from the extrapolated lower temperature flow tube measurements of Banerjee et al.[9] in the 1200-1250 K temperature range but the deviations increase at higher temperatures being as much as an order of magnitude at 1500 K. On the other hand the measurements for total decay rate coefficients by Bruinsma et al.[18] are an order of magnitude or more smaller than the current measurements over the temperature range 1200-1500 K. The recent recommendations by Baulch et al.[20] for $k_{-1a,\infty}+k_{-1b,\infty}$ appear to be lower by a factor of 2 (at

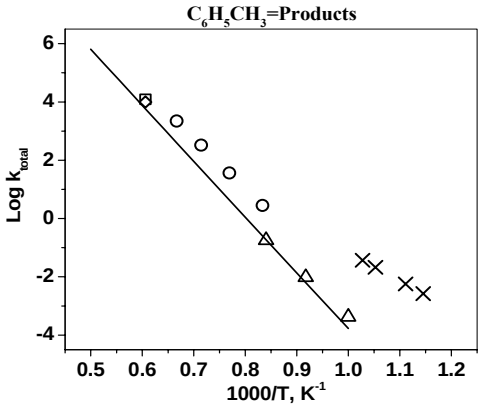

Fig 15: Comparison of Total Toluene Decay Rate Coefficients. [o] – This work[17] (1200–1500K), [□] – Kern et al.[13] (1650 K), [Δ] Bruinsma et al.[18] (1090-1190 K), [◊] – Eng et al.[19] (1650 K), [X] – Banerjee et al.[9] (875-975 K) [-] – Baulch et al.[20] (1000-2000 K).

1650 K) than the current measurements as well as the Eng et al.[19] and Kern et al.[13] recommendations with increasing deviations at lower temperatures (being as high as an order of magnitude at 1200 K). The total decay rate coefficients for the decomposition of toluene have also been used to extract production rate coefficients[17] for the formation of the dominant species in the current experiments viz. C_6H_6, CH_4, C_2H_2 and C_4H_2.

Despite a number of experimental and modeling studies on toluene dissociation at high temperatures there still exists discrepancies in several key features pertaining to its mechanism principal among them being the high temperature branching ratios for the primary decomposition steps. There are no direct thermal studies that have been able to isolate the two primary channels 1A and 1B in order to unambiguously extract rate coefficients. Consequently theory appears to be the only recourse. In recent work In recent work, Klippenstein et al.[21] have directly implemented multi-reference wavefunction based methods (MRCI/CASPT2) within variable reaction coordinate transition state theory (VRC-TST) for the key association reactions (1a, 1b) to yield a pressure dependent analysis of the primary rate coefficients in toluene decomposition over a wide range of temperatures (100-2658 K). The current experiments have been performed at high pressures and consequently we have utilized only the high pressure limiting rate coefficients from the Klippenstein et al.[21] calculations and refit their k_{1a} and k_{1b} over the temperature range 1027-1897 K by a modified Arrhenius expression to take into account the moderate temperature dependence that is exhibited for the two barrierless reactions. k_{-1a} and k_{-1b} are obtained over the same temperature range from these association rate coefficients via the equilibrium constants using the most recent thermochemical information for the benzyl radical[22] and the phenyl radical[23] for which the heat of formation is based on the recommendation by Davico et al.[24]. Apart from these initiation steps (-1a and -1b represent the primary dissociation steps for toluene) the chemical kinetic model that has been assembled to describe toluene pyrolysis includes key steps that describe abstraction reactions with H and CH_3, benzyl decomposition reactions, a benzene decomposition sub-mechanism, reactions that describe the formation and consumption of smaller hydrocarbons that range from methane to cyclopentadiene and reactions that describe the formation of key single ring aromatic soot precursors such as phenylacetylene and indene. The assembled model incorporating 87 species and 262

reactions (See ref. 17 for more details) was used to simulate our HPST experimental data (See Figure 16 below) as well as H atom profiles (Figures 17 and 18)obtained from prior toluene pyrolysis shock tube experiments[14, 19]. Despite a good agreement between the

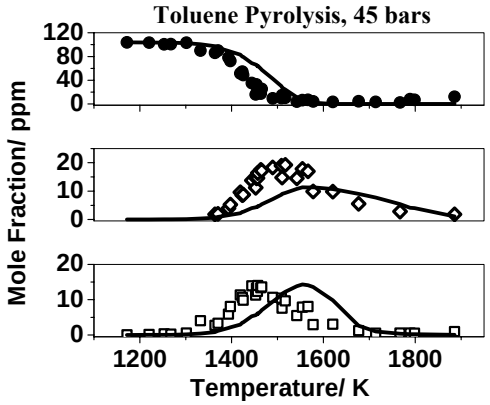

Fig 16: HPST Profiles Modeling [●] – $C_6H_5CH_3$, [□] - C_6H_6, [◊] – CH_4, [-] – Detailed Model.

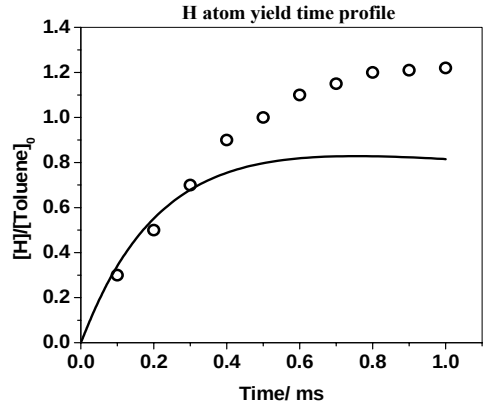

Fig 17: H atom modeling [o] – H atom Data from Ref. 19, Fig 3. T=1602 K, P=1.6 bar, $[Toluene]_0=1.2\times10^{-11}$ mol/cc.

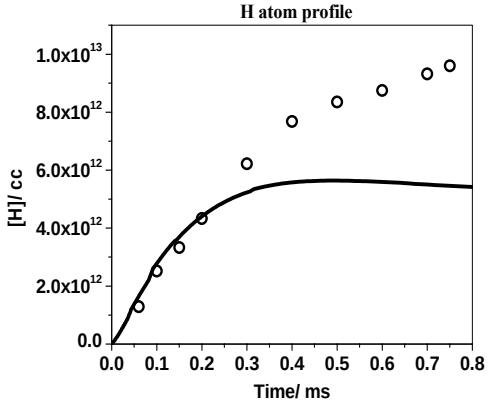

Fig 18: H atom modeling [o] – H atom Data from Ref. 14, Fig 4. T=1465 K, P=7.01 bar, $[Toluene]_0=4.2$ ppm.

model and the H atom profiles (Figures 17-18) in the short time scale regime (<300 μs) where the contributions are primarily due to only the two primary channels 1A and 1B the model appears to match the toluene decay profiles only moderately well and the peak methane mole fraction as well as the profile over the entire temperature range of the experiments is under predicted by a factor of 2 or larger. Sensitivity analyses for a typical 45 bar, 1500 K experiment (Figure 19) indicate that several key reactions play a major role in describing the toluene decay as well as benzene and methane growth. On the basis of a detailed uncertainty analysis[17] of the sensitive rate coefficients for these three species

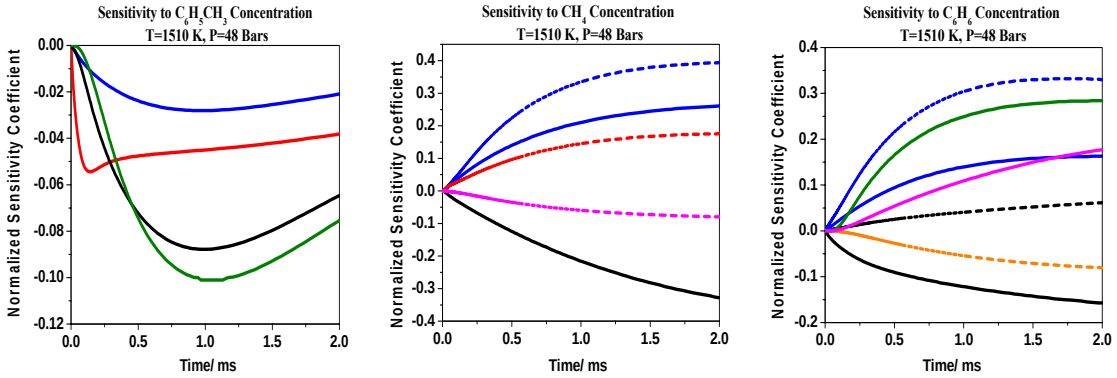

Fig 19: Sensitivity Analyses: [-]-H+$C_6H_5CH_2$=$C_6H_5CH_3$, [-]-CH_3+C_6H_5= $C_6H_5CH_3$, [-]-$C_6H_5CH_3$+H= $C_6H_5CH_2$+H_2, [---]-$C_6H_5CH_3$+H= C_6H_6+CH_3, [---]-$C_6H_5CH_3$+CH_3= $C_6H_5CH_2$+CH_4, [-]-$C_6H_5CH_2$=C_5H_5+C_2H_2, [-]-C_3H_3+C_3H_3=C_6H_6, [---]-C_6H_6=C_6H_5+H, [---]-C_6H_6+H=C_6H_5+H_2, [---]-$C_6H_5CH_3$+H= p-$C_6H_4CH_3$+H_2.

the only channel of consideration for the CH_4 profiles appears to be the primary channel 1A (association reaction 1a and the corresponding reverse dissociation reaction -1a). Since the association rate coefficient was determined from high level theoretical calculations the thermochemistry or more specifically the heat of formation for the phenyl radical plays a dominant role in determining the equilibrium constant for channel 1A (and consequently k_{-1a}) and consequently the heat of formation of phenyl was examined further. On the basis of a detailed analysis we have used an updated value for the heat of formation for phenyl (78.6 kcal/mole) that significantly improves the predictions to the HPST species profiles but worsens the predictions to the H atom profiles. Sensitivities to H atom profiles revealed that the only channel of consideration appeared to be channel 1B (apart from channel 1A which was updated based on the HPST profiles) that suggested a revision to the benzyl heat of formation (51.5 kcal/mol). The updated rate coefficients for channels 1A and 1B on the basis of the revised heats of formation for the two key radicals (phenyl and benzyl) now offers an excellent fit to the HPST species profiles (Figure 20) as well as the H atom profiles (Figures 21 and 22) under high pressure limiting conditions thereby validating the obtained high pressure limiting branching ratios between reactions -1a and -1b that range from 0.39-0.52 at T from 1200-1800 K.

The dominant intermediates from the pyrolysis of toluene[25] such as acetylene, diacetylene, benzyl, phenylacetylene and indene represent key soot precursors and consequently the description of the chemistry that leads to the formation and destruction of these species at high temperatures is critical to obtaining a fundamental understanding of the soot formation process. The soot precursor species profiles from the current

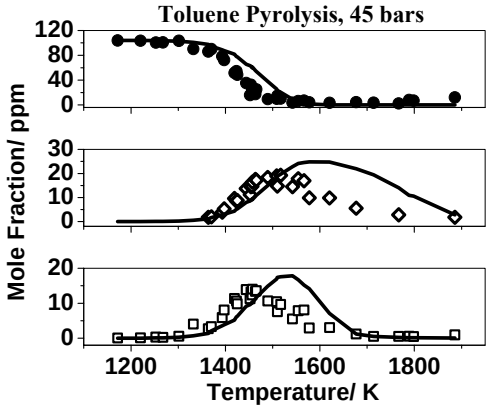

Fig 20: HPST Profiles Modeling [●] – $C_6H_5CH_3$, [□] - C_6H_6, [◊] – CH_4, [-] – Detailed Model with revised $\Delta H_f^0{}_{298K}$.

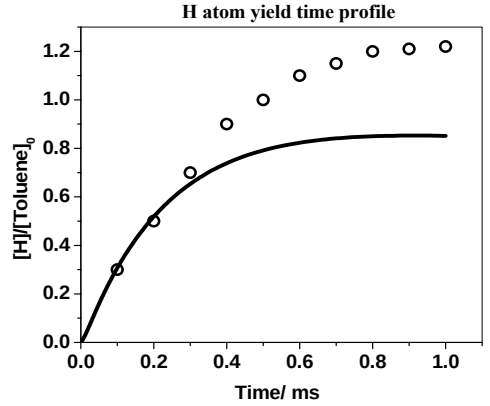

Fig 21: H atom modeling [o] – H atom Data from Ref. 19, Fig 3. T=1602 K, P=1.6 bar, $[Toluene]_0=1.2\times10^{-11}$ mol/cc.

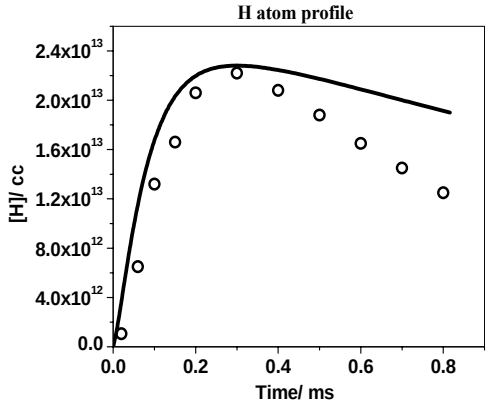

Fig 22: H atom modeling [o] – H atom Data from Ref. 14, Fig 5. T=1545 K, P=1.91 bar, $[Toluene]_0$=5.0 ppm.

experiments[25] represent key validation targets for the pyrolytic steps in large combustion models and consequently in this work we have tested mechanistic routes that describe aromatics growth and consumption on the basis of the HPST data.

The current high pressure toluene pyrolysis experiments yielded C_2H_2 which was the most dominant intermediate with mole fractions > 100 ppm. C_2H_2 starts to build up in significant amounts at temperatures below 1400 K which is definitive evidence for its formation from the decomposition of the benzyl radical albeit not via a direct unimolecular step. The formation of C_2H_2 from benzyl has been a source of uncertainty with multiple mechanisms proposed by several investigators. We have assembled a series of steps[25] as outlined by Laskin and Lifshitz[26] to describe benzyl decomposition in their shock tube study on the thermal decomposition of indene. The sequence of steps not only accounts for H atom formation but also explain C_2H_2 production from benzyl.

However this sequence of steps does not predict the HPST species profiles (Figure 23) and H atom profiles from recent benzyl decomposition experiments[27] (Figure 24). On the other hand utilizing two global decay steps for the benzyl radical as suggested by Colket and Seery[28] is able to account for both sets of data. It is clear from the current modeling exercise that the decomposition of benzyl is far from well characterized. We have attempted to explain the benzyl decay and acetylene formation by global steps. However it is very likely that benzyl decomposition involves the Laskin and Lifshitz[26]

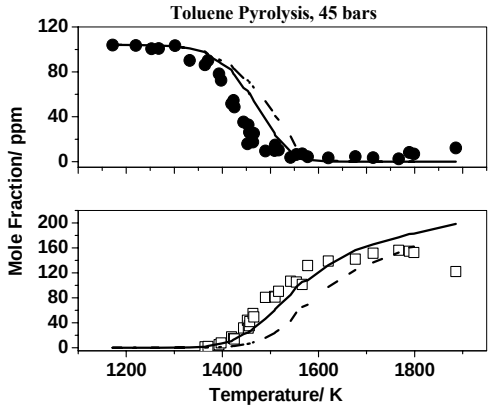

Fig 23: HPST Profiles Modeling [●] – $C_6H_5CH_3$, [□] – C_2H_2, [---] Model with Laskin and Lifshitz benzyl decay sequence. [-] – Model with global steps for benzyl decay.

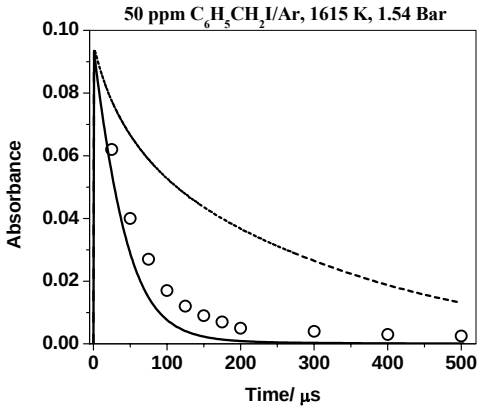

Fig 24: H atom modeling [o] – $C_6H_5CH_2$ data from Figure 2, Ref. 27. [---] –Model with Laskin and Lifshitz benzyl decay sequence. [-] –Model with global steps for benzyl decay.

sequence of steps as well as direct ring rupture. Detailed experiments that attempt to trap the intermediates that result from benzyl pyrolysis in combination with higher level ab-initio techniques and more sophisticated kinetic theories are required to shed light on the actual mechanistic processes by which benzyl decays as well as their associated rate parameters.

We have also modeled the profiles obtained for key soot precursor intermediates such as phenylacetylene (C_8H_6) and indene (C_9H_8) (See Figure 25 below). The sequence of steps used to describe the formation and decomposition of these species is mentioned in detail elsewhere[25]. Up to 85% of C_8H_6 is formed from the two channels $C_6H_5 + C_2H_2 \rightarrow C_8H_6 + H$ (54%) and $C_6H_5 + C_2H_2 \rightarrow C_6H_5CHCH$ (41%). These reactions are not only the two most dominant but also the most sensitive reactions. The majority of the indene (90%) is formed by the reaction c-$C_9H_9 \rightarrow C_9H_8 + H$ due to the large amounts of C_2H_2 and $C_6H_5CH_2$ (c-C_9H_9 is the stabilized adduct formed from the addition of benzyl and acetylene) present in these experiments with the remaining 10% produced by s-$C_9H_9 \rightarrow C_9H_8 + H$.

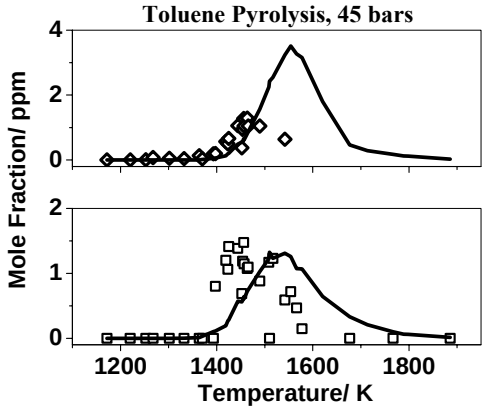

Fig 25: HPST Profiles Modeling 45 bars [◊] – C_8H_6, [□] – C_9H_8, [-] – Detailed Model[25].

The model is also able to predict the C_4H_2 concentrations fairly accurately at temperatures < 1550 K (See Ref. 25 for predictions). At higher temperatures the model over predicts the C_4H_2 formed in contrast to the experiments which depict a decay. However given the uncertainties with regard to the diacetylene chemistry the predictions appear to be reasonable. C_4H_4 profiles are fairly well reproduced by the model. However ethylbenzene and styrene concentrations are underpredicted whereas xylene concentrations are over predicted by the model. We have also estimated thermochemistry for the smaller aromatics and radicals in the model specifically for species not included in current databases[23] such as the C_9H_9 isomers using DFT calculations coupled with isodesmic correction schemes.

(d) Ethane Combustion:

Ethane is important both as fuel and as an industrial feed stock for the production of more valuable materials by pyrolysis or fuel rich oxidation, as in short contact time reactors. Consequently, it is desirable to have a reliable, comprehensive model for ethane combustion that can be used to accurately simulate processes over a wide range of

mixture stoichiometries, reactor temperatures and pressures. Such a model would have to be developed in conjunction with a good, self consistent set of experimental data that incorporates conditions found in real reactors such as high-pressures and temperatures. Until fairly recently the upper pressure limit of experimental data reported in the literature for ethane oxidation and pyrolysis at high temperatures was around 10 bar with most experiments conducted at 2 bar or less. The experimental work performed here at UIC has obtained data over a pressure range spanning 5 bar at the low end, which is close to the upper limit of most other chemical shock tubes, and up to 1000 bar at the high end, beyond the pressure capabilities of other chemical shock tubes. The experimental study of ethane combustion[29-31] spans P=5-1000 atm, T=1000-1500 K, oxidation (Φ=1, 5) and pyrolysis. Much of the higher pressure data[29, 30] has been discussed in detail in prior DOE annual reports. The experimental work in this annual period has been extended to pressures as low as 5 atm and the entire data set has been simulated with a single comprehensive chemical kinetic model[31] that can capture the experimental trends over the wide range of pressures, temperature and stoichiometry.

The comprehensive model developed in this study referred to as the modified Miller model used the Miller 2001[32] model as a basis. The changes made to this model are described in more detail in the relevant publications[30, 31]. The predictive capability of the widely used GRI-Mech 3.0[33] was also tested against the entire data set. Figure 26 depict representative profiles for ethane and the predictions of the developed modified Miller model, the base Miller model and GRI-Mech 3.0 to the data. In general the

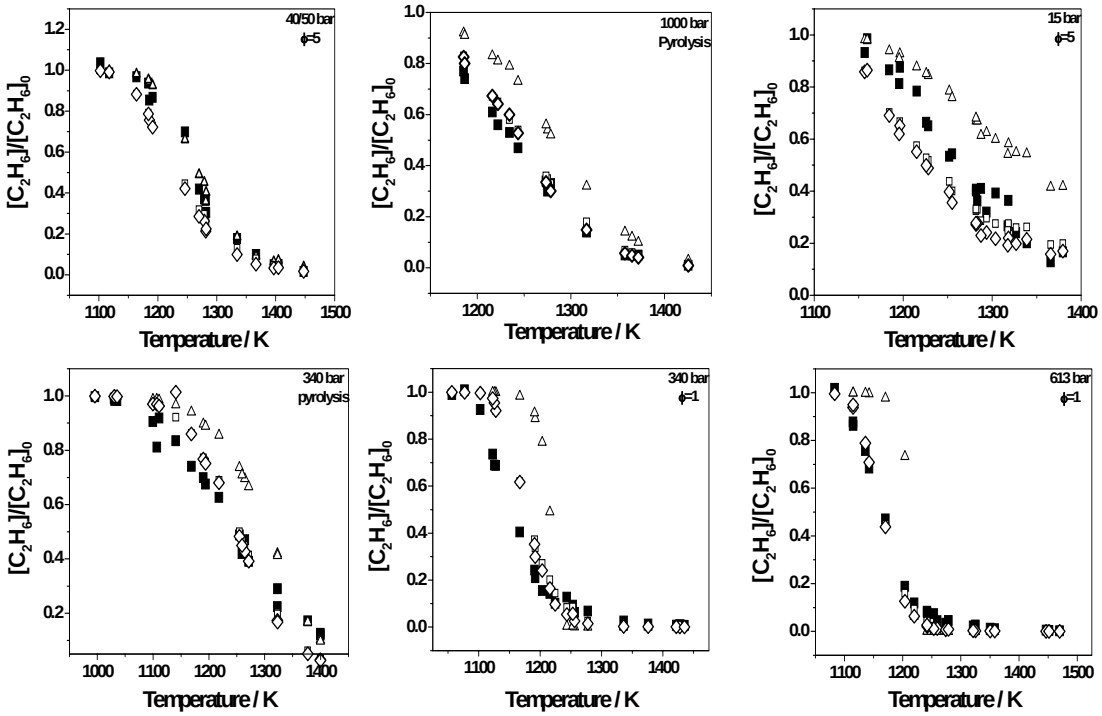

Fig 26: Ethane Combustion, [■] – Data, [Δ] – GRI-Mech 3.0, [□] – Miller Model, [◊]- Modified Miller Model.

predictions for the modified Miller model are good over the entire T, P and Φ regime. Similar good predictions are also observed for other primary intermediates C_2H_4, C_2H_2, CO and products CO_2, observed in this study. The modified Miller model also is able to simulate 1 atm JSR species profiles from the work of Bakali et al.[34]. The model also

makes good predictions of ignition delay measurements reported by Bakali et al.[34] and Hidaka et al.[35].

(e) PAH Thermochemistry:

Thermochemical and molecular properties are critical parameters in many aspects of gas kinetics and the accuracy to which these parameters are determined can greatly affect the determination of a variety of parameters including rate coefficients, rates of heat release and branching ratios, all of which are critical in the accurate simulation of reactive gas phase systems. It is essential that values of $\Delta H_{f\ 298\ K}^{0}$ be obtained to an accuracy within 2 kcal/mol for situations where it is not possible or difficult to obtain good experimental data for multichannel reactions or for the estimation of rate coefficients. For PAHs there are very limited reliable measurements for $\Delta H_{f\ 298\ K}^{0}$ and the majority of the reported data are for species with a maximum of four rings. The difficulty of performing these measurements makes theoretical methods for determining heats of formation for large aromatics and PAHs attractive if the calculations can be performed with sufficient accuracy so as not to introduce excessive errors into subsequent kinetic calculations.

The development of very fast and affordable computers with large storage/memory capacities have contributed to the rapid development of ab-initio methods that are able to increasingly replicate experimental accuracies for molecular properties and kinetics. Higher level theoretical methods that incorporate electron correlation to estimate molecular energies with greater precision have been developed that include the G2[36], G3[37] and CBS-Q[38] composite methods and these methods have been used to estimate heats of formation that have mean absolute deviations herewith referred to as MAD from the experimental heats of formation < 2 kcal/mol for a large set of common hydrocarbon molecules having as many as six carbon atoms. These high level methods become very expensive to use for large molecules with several heavy atoms due to time and memory requirements and are at present not suitable for routine application to large systems such as PAHs particularly when it is necessary to obtain thermochemical information for a large number of species. Thus a method of estimating heats of formation for PAHs that does not require time consuming calculations and that is usable beyond the test group of species has been developed. The method that we refer to as ring conserved, RC, isodesmic reactions[39], makes use of inexpensive DFT methods to obtain heats of reaction and has been used to accurately estimate the heat of formation for molecules as large as 9, 10 - diphenylanthracene ($C_{26}H_{18}$).

The DFT calculations reported in this work[39] were performed using the Gaussian 98 series of programs[40]. Input structures for the molecules were generated using the CHEM3D[41] software that is part of the CHEMOFFICE suite. The B3LYP functional with the 6-31G* basis set was used for the geometry optimizations. This level of theory is shown to be adequate for obtaining accurate molecular geometries, vibrational frequencies and zero point energies and is used for these computations in composite methods such as the G3B3 method[42]. Furthermore taking into account the large molecular systems involved it is at present viable to employ only this level of theory. Frequency calculations were performed on the optimized geometries at the same level of theory to confirm that the structures were minima on the potential energy surface and also to obtain the vibrational frequencies and thermal corrections essential for the evaluation of the

molecular partition functions. $\Delta H_f^0{}_{298K}$ were extracted from the DFT (B3LYP/6-31G*) energetics using the procedure outlined by Notario et al.[43] with the only difference being in the treatment of the vibrations in the calculation of the integrated heat capacity [$\Delta H_{Vib}(T)$]. A scaling factor of 0.9989 is applied to the calculated frequencies as recommended by Scott and Radom44 and a low frequency vibrational scaling factor (1.0013) was applied for frequencies less than 625 cm^{-144}. Furthermore to account for internal rotations frequencies less than 260 cm^{-1} are treated as free rotors with a contribution of RT/2 to $\Delta H_{Vib}(T)$[45].

Theoretical $\Delta H_f^0{}_{298K}$ for the species of interest can be estimated from a variety of reaction schemes in which the experimental $\Delta H_f^0{}_{298K}$ for the other species in the reaction are known to a high degree of accuracy. An atomization reaction represents the simplest of these schemes and is often the reaction scheme of choice when molecular energies are estimated to a high level of precision using composite methods such as the G3B3 method[42]. However when molecular energies are estimated using low level theoretical methods such as the one employed in this work atomization reactions lead to large errors in the computed $\Delta H_f^0{}_{298K}$.

Hehre et al.[46] have shown that errors that accumulate due to incomplete capture of electron correlation energy when using low level theory cancel when utilizing bond separation, BS, isodesmic reactions in which the molecular nature of the species of interest is retained in the products. In BS isodesmic reactions, the number and type of bonds are retained. Recently Raghavachari et al.[47] utilized this BS isodesmic scheme using higher level (G2 and G2MP2) methods to evaluate $\Delta H_f^0{}_{298\ K}$ for a large number of small species using a simple set of nine reference molecules with well characterized experimental heats of formation (uncertainty~0.1 kcal/mol).

In general the use of an isodesmic reaction scheme leads to more effective cancellation of errors in computing enthalpies of reaction than atomization reactions or group additivity methods. However as has been demonstrated by Petersson et al.[48] the application of bond separation isodesmic reactions to the estimation of heats of formation for large molecules such as PAHs can lead to excessively large errors in the estimated value simply due to the large number of molecules involved in the isodesmic reaction. This is illustrated by reaction 1.

$$C_{10}H_8 + 12CH_4 \rightarrow 6C_2H_6 + 5C_2H_4 \qquad (1)$$

An error of 0.5 kcal/mol for each of these molecules could lead to a net error of 12 kcal/mol in estimating a heat of formation. Petersson et al.[48] argue that the good agreement observed by Raghavachari et al.[47] between the calculated and experimental $\Delta H_f^0{}_{298\ K}$ for naphthalene by reaction 1 is fortuitous and they suggested that a more appropriate reaction for naphthalene would be reaction 2,

$$C_{10}H_8 + C_2H_4 \rightarrow 2C_6H_6 \text{ (Benzene)} \qquad (2)$$

The $\Delta H_f^0{}_{298\ K}$ of benzene is known to 0.1kcal/mol accuracy and Petersson et al. suggest that benzene should be included as a reference species for isodesmic reactions.

In evaluating the isodesmic reaction scheme Petersson et al. do not suggest a common methodology that can be applied to heavier aromatic systems. This is due to the fact that in such reaction schemes a number of isodesmic reactions can be applied to a single molecule when determining ΔH_r (Heat of Reaction). For example in the case of anthracene several different isodesmic reactions can be generated such as using one (3),

two (4) or three C_6H_6 (5) molecules each "conserving" one, two and three aromatic rings respectively.

$$C_{14}H_{10} + 12CH_4 \rightarrow 6C_2H_6 + 4C_2H_4 + C_6H_6 \quad (3)$$

$$C_{14}H_{10} + 6CH_4 \rightarrow 3C_2H_6 + C_2H_4 + 2C_6H_6 \quad (4)$$

$$C_{14}H_{10} + 2C_2H_4 \rightarrow 3C_6H_6 \quad (5)$$

The question would then arise as to which isodesmic reaction should be used to estimate $\Delta H_f^0{}_{298\,K}$. On the basis of the least number of molecules involved as per the argument of Petersson et al. reaction 5 would be the appropriate choice. However this is not the most accurate solution and for aromatic systems a different scheme is required to that used for simple hydrocarbons.

The new scheme referred to as a Ring Conserved, RC, Isodesmic Reaction Scheme[39] indirectly accounts for the resonance or delocalization energy of the aromatic or PAH molecule of interest. The RC isodesmic reaction scheme involves the use of isodesmic reactions that closely match the aromatic nature of the PAH or aromatic species of interest. To account for the resonance energy we have utilized a simple protocol based on a recent formula developed by Wiberg[49]. Wiberg studied the structural properties and energetics for a set of linearly annelated PAHs (benzene through pentacene) and a set of angularly annelated PAHs (phenanthrene, chrysene and picene). Using the thermochemically derived stabilization or resonance energies for benzene (36 kcal/mol) and naphthalene (60 kcal/mol) Wiberg was able to obtain a relation for the delocalization energies in the heavier molecules based on energies obtained from DFT calculations at B3-LYP/6-311G** level of theory. The delocalization energy (kcal/mol) as defined by Wiberg is

$$E_{Delocalization,\,M} = 627.5*[E_M + (-E_{C6H6,\,R}) + (n-1)*(E_{C6H6,\,R} - E_{C10H8,\,R})] \quad (6)$$

E_M represents the calculated energy (Hartrees) of the molecule of interest obtained using DFT (B3-LYP/6-31G* used in present work), $E_{C6H6,\,R}$ (-231.509849 Hartrees) is the DFT energy for benzene corrected for its resonance energy (36 kcal/mol), $E_{C10H8,\,R}$ (-385.797112 Hartrees) is the DFT energy for naphthalene corrected for its resonance energy (60 kcal/mol) and n represents the number of rings in the molecule. The above relation was used to determine the delocalization energies, Table I, for the molecules using B3-LYP/6-31G* level of theory which is relatively inexpensive for these large molecules. The delocalization energy per π bond (C=C) was also determined and is presented in Table I.

Table I: Delocalization Energies at B3-LYP/6-31G*

Molecule	Rings	Energies (Hartrees)	Delocalization Energy (kcal/mol)	Delocalization Energy/C=C (kcal/mol)
Benzene	1	-231.5672198	36.00	12.00
Naphthalene	2	-385.8927297	60.00	12.00
Anthracene	3	-539.5305236	80.05	11.44
Naphthacene	4	-693.1658125	98.54	10.95
Pentacene	5	-846.7999436	116.30	10.57
Phenanthrene	3	-539.5386567	85.16	12.17
Chrysene	4	-693.1819395	108.66	12.07
Picene	5	-846.8261576	132.74	12.07
			Mean	11.66

These delocalization energies per C=C have been used to determine the number of rings to be conserved to preserve the aromaticity of the parent molecule when constructing the isodesmic reactions. This technique automatically identifies a unique isodesmic reaction for any PAH molecule and these reactions are referred to as the RC isodesmic reaction for that particular molecule. In line with Wiberg's observation the delocalization energy per C=C remains almost constant for the angularly annelated arenes whereas for the linearly annelated arenes there is a small decrease as the size of the molecule increases (Table I). The average delocalization energy based on B3-LYP/6-31G* calculations per C=C for this test set of eight molecules is 11.66 kcal/mol. This value can be used to determine the delocalization energy for any PAH by simply determining the number C=C bonds in the aromatic part of the molecule. For example in the case of naphthalene the number of C=C is 5 and the net delocalization energy is 58.30 kcal/mol (5*11.66 kcal/mol), which is close to the 60 kcal/mol calculated from equation 6. In comparison with the delocalization energy for benzene (36 kcal/mol) the net delocalization energy for naphthalene is 1.67 times that of benzene (60/36). This implies that a reaction which "conserves" two benzene molecules (reaction 2) would be able to more closely represent the delocalization energy contribution to naphthalene than a scheme that conserves only one ring and hence a more complete cancellation of systematic errors that accumulate because of the method and the small basis set used is achieved. However in the case of the larger PAH molecules, for example anthracene the Petersson et al.[48] scheme (reaction 5, decomposition of 3 benzene rings) does not result in complete correlation energy cancellation. Anthracene has 7 C=C and hence its net delocalization energy is 81.62 kcal/mol close to the result from equation 9 of 80.05 kcal/mol. This is approximately 2.22 times the delocalization energy for benzene (80.05/36) and hence a reaction conserving two benzene rings (reaction 4) instead of three benzene rings would lead to better cancellation of errors.

This simple protocol for estimating delocalization energies was shown by Wiberg [49] to be valid for cata-condensed PAHs such as those in Table 1. However the use of the simple formula to estimate the delocalization energy which is subsequently used to identify a unique RC isodesmic reaction for any general aromatic or PAH molecule leads to very good predictions of experimental $\Delta H_f^0{}_{298\,K}$ for a test set of 37 aromatic and PAH molecules with well defined experimental measurements. Table 2 is a compilation of the molecules used in the test set as well as the predictions made by the new scheme. The majority of the experimental measurements for comparison were taken from the NIST database[50] unless otherwise mentioned and a more detailed discussion of the sources for the experimental data can be found in a related publication[39]. Detailed information including the ab-initio energies, vibrational frequencies as well as a more detailed discussion of the scheme can be found in the same article[39]. The new RC isodesmic scheme predicts the experimental $\Delta H_f^0{}_{298\,K}$ with a Mean Absolute Deviation [MAD] of 1.14 kcal/mol for the 37 molecules with well defined experimental measurements and a MAD 1.71 kcal/mol for the entire set of 55 species. In general the large majority of molecules have absolute deviations less than 2 kcal/mol. Furthermore within the test set as the size of the molecule increases from single ring aromatics to condensed PAH systems with as many as five rings no apparent increase in absolute deviations from experimental values is observed.

The RC isodesmic scheme is able to make good predictions with a MAD of 1.14 kcal/mol for a wide range of aromatics and PAHs using energetics from low level, cost effective DFT (B3LYP/6-31G*) calculations. However current state of the art thermochemical methods such as the high level composite methods (Gn and CBS family of methods) are able to achieve MADs less than 1 kcal/mol which is termed "chemical accuracy" and is often the reported accuracy for experimental measurements. In order to further validate the new scheme presented here and improve its predictions a correlation scheme was utilized[51]. Figure 27a is a depiction of the correlation between the calculated (RC) and experimental $\Delta H_f^0{}_{298\ K}$. There is an excellent correlation (R^2=0.9994) between the experimental and the RC calculated $\Delta H_f^0{}_{298\ K}$.

The excellent correlation observed for the new scheme offers good support for its validity and such a correlation can also be used to further minimize the observed errors. Equation 7 represents the correlation between the experimental and calculated $\Delta H_f^0{}_{298\ K}$ for the 37 molecules with well established experimental $\Delta H_f^0{}_{298\ K}$.

$$\Delta H_f^0{}_{298\ K,\ Calculated} = 0.9791 * \Delta H_f^0{}_{298\ K,\ Experimental} + 1.57318 \quad (R^2=0.9994) \qquad (7)$$

If equation 7 is used to scale the DFT//RC calculated $\Delta H_f^0{}_{298\ K}$ for the test set of 37 molecules then the mean absolute deviations for the test set drops to 0.88Kcal/mol which is excellent and well within the limits of "chemical accuracy". The correlations are also used to scale the calculated $\Delta H_f^0{}_{298\ K}$ for the other 18 molecules with uncertain experimental measurements and the MAD for the entire set of 55 molecules is 1.48 kcal/mol. Among the entire set of molecules only corannulene and benzo(k)fluoranthene show large deviations in line with the predictions made by Yu et al.[52] who have suggested a review of the experimental measurements is necessary for these two molecules. The MAD for the 53 species excluding the above two species is 1.16 kcal/mol. None of the other molecules show deviations larger than 4 kcal/mol and among the 37 molecules with well defined experimental measurements none of the molecules have a deviation larger than 3 kcal/mol and for 90% of the species $\Delta H_f^0{}_{298\ K}$ are predicted to be within 2 kcal/mol indicating that the present method has very few outliers beyond the acceptable accuracy of 2 kcal/mol. Figure 27b shows the distribution of errors from experimental measurements for the test set of 37 molecules and in general a large majority of the molecules lie within the ±2 kcal/mol range.

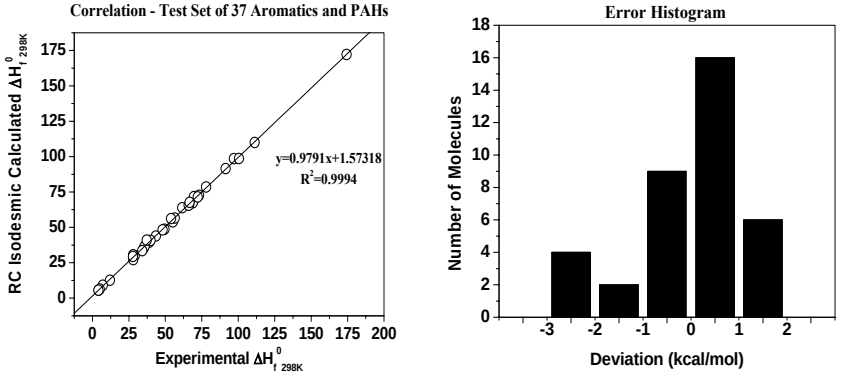

a **b**

Fig 27: PAH Thermochemistry a. Correlation between experimental and calculated $\Delta H_f^0{}_{298\ K}$. b. Error distribution.

As an additional test this newly proposed RC isodesmic scheme is compared against the optimized homodesmic reaction scheme developed by Yu et al.[52] which has been used to obtain estimates for $\Delta H_f^0{}_{298\ K}$ for a large number of PAHs. In this optimized scheme which forms part of a recent publication by Yu et al.[52], a new bond centered group additivity scheme has been developed to estimate the thermochemistry of PAHs. Yu et al.[52] have evaluated the use of several reaction schemes, atomization, BS isodesmic as well as four types of homodesmic reaction schemes to estimate heats of formation using ab-initio molecular energies computed at B3LYP/6-31G(d) level of theory for a training set of 15 PAHs with well known experimental $\Delta H_f^0{}_{298\ K}$. The primary training set of 15 molecules includes only cata and peri-condensed PAHs but Yu et al.[52] have also evaluated the use of their reaction schemes to predict $\Delta H_f^0{}_{298\ K}$ for C_{60} and C_{70} fullerenes. Yu et al.[52] concluded that a homodesmic reaction scheme (optimized scheme) with benzene, naphthalene, phenanthrene and 1/12 C_{60} as reference molecules performed the best in predicting $\Delta H_f^0{}_{298}$ for the 15 molecules as well as C_{60} and C_{70}. The Yu et al.[52] predictions and a comparison against the predictions made by the RC isodesmic reaction scheme has been included for their test set. The MAD for the training set of 15 molecules is 1.4 kcal/mol with no further increase in MAD when including C_{60} and C_{70}. However in evaluating the MAD for the training set of 15 molecules they have also included the reference molecules benzene, naphthalene and phenanthrene for which the errors would obviously be zero. The actual MAD for the test set of 12 molecules excluding the reference molecules is 1.9 kcal/mol using their homodesmic reaction scheme and 2.9 kcal/mol when their group additivity scheme is used. In comparison the RC isodesmic reaction scheme has a MAD 2.0 kcal/mol for the entire set of 15 molecules. The MAD is 2.1 kcal/mol when the reference molecule is excluded from the set and this is very close to the MAD of 1.9 kcal/mol obtained by the Yu et al.[52] homodesmic scheme and is an improvement from the predictions made by their group scheme which has a MAD of 3.4 kcal/mol. Furthermore Yu et al.[52] have restricted their reaction scheme to cata and peri-condensed PAHs and have not tested it against substituted aromatics and PAHs. The proposed RC isodesmic reaction scheme includes only benzene as the aromatic reference molecule (which has a well characterized $\Delta H_f^0{}_{298}$) without compromising the accuracy that is obtained by the optimized homodesmic reaction scheme proposed by Yu et al.[52]. The authors are aware that the current scheme has its limitations in that it does not account for structural parameters such as ring strain and H-H repulsion which are significant contributors when considering large floppy PAH molecules. However considering the simplicity of the current non-parametrized method, its performance (less than 2 kcal/mol MAD) for a general test set of varied aromatics and PAHs justifies its usage and applicability to larger set of aromatic and PAH molecules with unknown experimental $\Delta H_f^o{}_{298K}$.

(f) Shock Tube Characterization:

The primary concerns when using a shock tube as a reactor for chemical kinetic studies are the determinations of reaction temperature, pressure and residence time since kinetic simulations depend heavily on them. There are standard techniques for determining these parameters that are widely used by shock tube practitioners[29, 53-64]. For a single pulse shock tube[29, 53-57], normally the reaction pressure is approximated by an averaged pressure based on the measured endwall pressure trace, the reaction temperature

is assumed to be constant and either analytically calculated from classic shock tube equations or experimentally calibrated using a chemical thermometer, and the reaction time is empirically assigned as either the dwell time at which the pressure begins to fall or as the residence time at which the pressure falls to 80% of its highest value. However in most realistic situations temperature, T_5, and pressure, P_5, behind reflected waves in a shock tube are not constant as normally assumed, particularly in a single pulse HPST, and experience non-uniform time distributions as suggested by Figure 28, an endwall pressure trace in the single pulse high pressure shock tube (HPST) at The University of Illinois at Chicago.

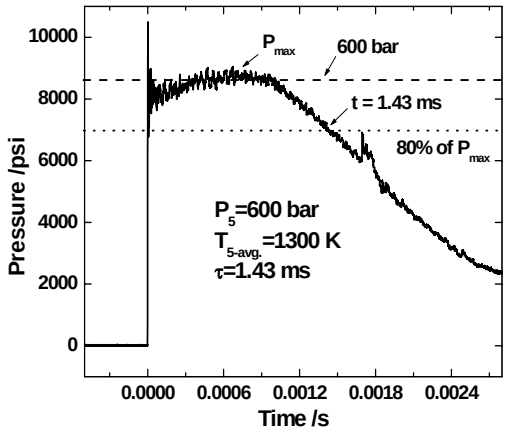

Fig 28: Typical endwall pressure trace at 600 bar. In this particular case, kinetic simulation inputs to Chemkin are P = 600 bar, T = 1300 K and τ = 1.43 ms. Note the $T_{5\text{-avg}}$ was experimentally calibrated using a chemical thermometer.

To characterize the variations with time, numerous investigations have been conducted and considerable progress has been made[29, 58-61]. Currently it is generally agreed that the non-ideality is the consequence of both the choice of operating conditions and also the physical construction of the shock tube itself. The compressible fluid mechanics that are related to both the operating conditions and the tube construction are responsible for boundary layer development in the shock tube which impacts, in a very complex way, the achieved temperature and pressure especially in those tubes with dump tanks. In spite of the complexity, the biggest uncertainty in temperature, T_5, can be approximated by quantitative deduction based on an isentropic assumption using experimentally measured pressure traces. In this manner, Peterson and Hanson[58] have recently investigated non-ideal behavior of the HPST at Stanford and found that the temperature increase, ΔT_5, can be up to 85 K at 100 atm and 1800 K (Fig. 8 in ref 58). A logical question stimulated by their result is whether the use of a time independent temperature, as is commonly done in single pulse shock tube experiments, is suitable in kinetic simulations without causing significant errors.

Another question that arises from the time varying nature of the reaction temperature is whether or not reactions taking place during the quenching period, the time when the pressure and temperature are dropping after the pressure plateau has been reached, will affect measured species concentrations in a way that significantly impacts the simulation of those concentrations. Despite the assumption that reactions stop immediately as soon as the pressure and temperature drop, it has been suspected for a

long time that reactions will continue as reacting hot gas cool down over a finite time interval. A counter argument to the suspicion that reactions continue is that reactions with high activation energies will stop immediately but only relatively unimportant reactions with low barriers and barrierless reactions will be continuing. However, if in fact many reactions do continue during the quenching period, then the empirical way of reaction time assignment needs to be carefully examined since the quenching process usually lasts a few milliseconds, approximately the same time scale as the assigned reaction time. Accounting for reactions that continue during the quenching process if they were important, however, is not a trivial task because not only temperature as function of time has to be obtained for the modeling but also a change in current modeling programs has to be made to allow integration of the kinetic equation using both time dependent pressure and temperature. Despite the difficulty involved, Colket and co-workers[62, 63] addressed quenching effects when simulating kinetics behind reflected shock waves at about 8 atm. Unfortunately, in their work the initial endwall temperature $T_5(0)$, which is the basis for the deduction of the temperature trajectory, was calculated by the classic shock equations from the measured Mach number[64], a method apparently problematic when applied for HPST according to the study by Davidson and Hanson[59]. A more accurate way to model and evaluate the role of reactions during quenching would be to first obtain from experimental calibration a $T_{5\text{-avg}}$ and then to back deduce T_5 (0) and time dependent T_5 traces. With time dependent T_5 and P_5 traces, kinetic simulations can be performed to determine if reactions continuing during quenching are significant.

One last concern, even if time dependent T_5 and P_5 and quenching process are all accounted for, is real gas effects when utilizing the shock tube to explore kinetics at high pressures. At very high pressures, the ideal gas equation of state (EOS) is inadequate to describe the P-V-T behavior of the mixture behind reflected shock waves. A half century ago Beatie[65] developed a general methodology to incorporate an EOS into the calculation of non-ideal thermodynamic properties. Based on Beatie's methodology, a computer program called Chemkin Real Gas was developed by Schmitt, Butler and French[66] that contains a problem-independent set of subroutines capable of calculating thermodynamic properties and reaction rates based on cubic types of EOS. The Chemkin Real Gas program could provide a good stage to study real gas impacts on the development of a comprehensive kinetic model, but, to the best of our knowledge, no such work has been reported so far.

Therefore it would seem important to evaluate when developing or validating chemical kinetic models based on single pulse shock tube data the effects of (1) time dependent temperature and pressure variations in contrast to assuming constant temperature and pressure, (2) inclusion of reactions during quenching by cooling in contrast to the assumption of zero kinetic contributions and (3) real gas behavior in contrast to assuming ideal gas conditions. The evaluations of these potential effects via numerical simulations are the subject of this study[67] aimed to better characterize the UIC HPST.

Based on an isentropic assumption, the time dependent endwall temperature T_5 was deduced from measured pressure traces and the calibrated temperature $T_{5\text{-avg}}$. A finite difference approximation method was employed to discretize the kinetic integration range into small subsections where constant reaction pressure can be assumed. Chemkin[68] was modified to carry out the integration with time varying temperature, pressure and

compositions. To assess real gas impacts, the Chemkin Real Gas subroutine library[66] was implemented with Senkin[69] forming RG-Senkin, a program capable of performing the same job Senkin does but with multiple choices of cubic EOS to evaluate real gas impacts on chemical kinetics. The computational approaches involved in describing the effects of real gas under high pressures are

1. Treatment of the forward rate constant as conventional TST ideal gas rate constant for simplicity and due to lack of information on activation volume ΔV.
2. Correction of P-V-T relationship - Employing the Peng-Robinson cubic EOS.
3. Correction of thermodynamic properties (H, S, Cp) for real gas EOS.
4. Correction of reverse rate constant via fugacity coefficients calculated in step 3.
5. Definition of governing boundary conditions – Constant pressure adiabatic isenthalpic system (Defines condition behind a reflected shock wave)

The numerical techniques employed are described in more detail elsewhere[67, 70].

The RG-Senkin developed as part of this study[67] was used to calculate the time dependent endwall temperature $T_5(t)$ obtained from the observed pressure traces $P_5(t)$ and the calibrated temperature $T_{5\text{-avg}}$ in the time interval from when reflected shock wave arrives (reaction starts) to when the pressure drops to its 30% highest value. The reason we limit our efforts to this range is that all reactions stop within this range, a phenomena that will be demonstrated later in this article. Figure 29 represents an end-wall pressure profile for a 600 bar shock with a $T_{5\text{-avg}}$ 1300 K obtained from chemical calibration using 1,1,1-trifluoroethane. In the computational experiment with the 600 bar shock shown in Figure 29, we examined real gas effects by utilizing the Peng-Robinson equation of state with a stoichiometric 200 ppm ethane-oxygen mixture diluted in argon. It is found that the differences in T_5 calculated using the ideal gas equation with the one from the real gas equation of state are barely discernible even at this high pressure. The almost identical T_5 trajectories tend to imply that the non-ideality of temperature behind reflected shock waves may be largely caused by the non-ideal fluid mechanics and the non-ideality of thermodynamic properties of this particular reaction system at such temperature and pressure may be insignificant. Our computed temperature increase from the experimentally measured pressure profile and calibrated temperature in the UIC HPST is in a very good agreement with that of the Stanford HPST wherein they observed[58] an endwall temperature increase of $\Delta T_5 = 20–45$ K at t = 500 μs. In our work[67], we have

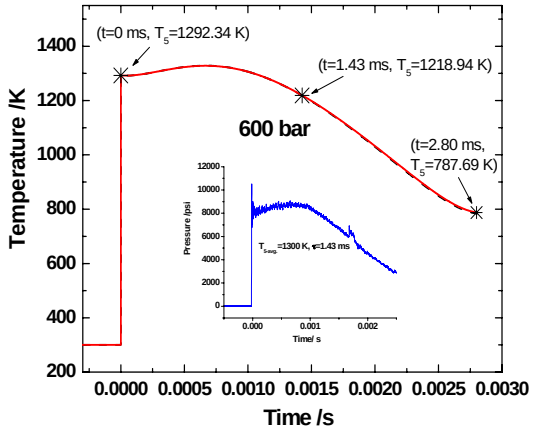

Fig 29: Computed endwall temperature T5 as a function of time at nominal 600 bar with a test gas of stoichiometric mixture of 0.002% C_2H_6–0.007% O_2–Ar. In the temperature plot, solid line: ideal gas equation of state, dashed line: Peng-Robison equation. The difference is barely discernible. Plotted in the figure also is the pressure traces used for T_5 deduction.

defined an average quenching rate as the temperature change rate in the time range from the point at which pressure falls to its 80% highest value (where reaction time was empirically taken) to the point where a smooth pressure profile ends. Using this definition, the calculated quenching rate of UIC HPST was found to be 3.02×10^5 K/sec for the 600 bar shock which is almost half of Lifshitz's[71] estimate probably in a large part because of the different physical construction of the shock tubes.

Tsang[53] has examined the possible error introduced by the use of mean reaction temperature and reaction time assignment in the study of unimolecular reactions. However, the focus here is to assess the kinetic impacts on a full detailed chemical kinetic model of time dependent T_5 and P_5 as well as finite reaction quenching on much more complicated reaction systems. To approach the assessment, we have chosen a detailed chemical kinetic model of toluene oxidation which has been recently developed in our laboratory[1] from HPST data and validated by flow reactor data. A stoichiometric mixture ($\Phi = 1$) of 0.002% C_7H_8–0.018% O_2–Ar was used as reagent. With the calculated temperature trace for the 600 bar shock as described earlier, kinetic simulations were performed using time dependent P_5 and T_5 throughout the whole reacting and quenching periods. The results were then compared with those obtained by the conventional treatment of using constant $T_{5\text{-avg}}$, P_5 and an empirically assigned reaction time τ as input. The stable species measured in our HPST experiments were chosen as the primary Chemkin output information. Considerable attention was also given to key radicals H, CH_3 and OH because these radical species play very important roles in chain reactions and because they serve frequently as the experimental target during shock tube studies such as when hydroxyl radicals are used in an ignition delay time study and hydrogen atoms in atomic resonance absorption spectrometric (ARAS) detection.

Figure 30 presents the comparative results of species mole fraction with C_7H_8 and C_2H_6 in panel (a), C_2H_2 and C_6H_6 in panel (b) and H, CH_3 and OH radicals in panel (C). The predicted concentrations of stable species using constant T_5 and P_5 are quite close to the predictions using corrected T_5 and P_5 at t = 1.43 ms when pressure drops to 80% of its highest value and at which point the reaction time was empirically taken. When reaction quenching is considered, the stable species populations are still changing but only slowly. Also seen in panels (a) and (b) of Figure 30 is that at t = 2.0 ms and T_5 = 1038 K at which time the pressure has dropped to 50% of its highest values, the stable species are no longer changing concentration. Therefore, for this particular case, the overall error associated with the adoption of constant T_5 and P_5 and an empirically chosen τ at the time of 80% of the pressure maximum, through comparison with the corrected predictions with time dependent T_5 and P_5 and accounting for reactions during quenching, is less than 10% for C_7H_8 and C_2H_6 and less than 5% for C_2H_2 and C_6H_6. Discrepancies, however, become pronounced for radical species as is clearly seen in panel (c) of Figure 30. The predicted mole fractions for these species with the assumption of constant T_5 and P_5 are as much as double those predicted by using time dependent T_5 and P_5 at t = 1.43 ms. Moreover, their populations continue to change dramatically during the reaction quenching period until all of them are consumed.

To further investigate the impact of continued reactions during the quenching period, particularly how concentrations are altered, we chose C_7H_8 and C_2H_6 as target species and performed reaction pathway analysis to identify the most important reactions

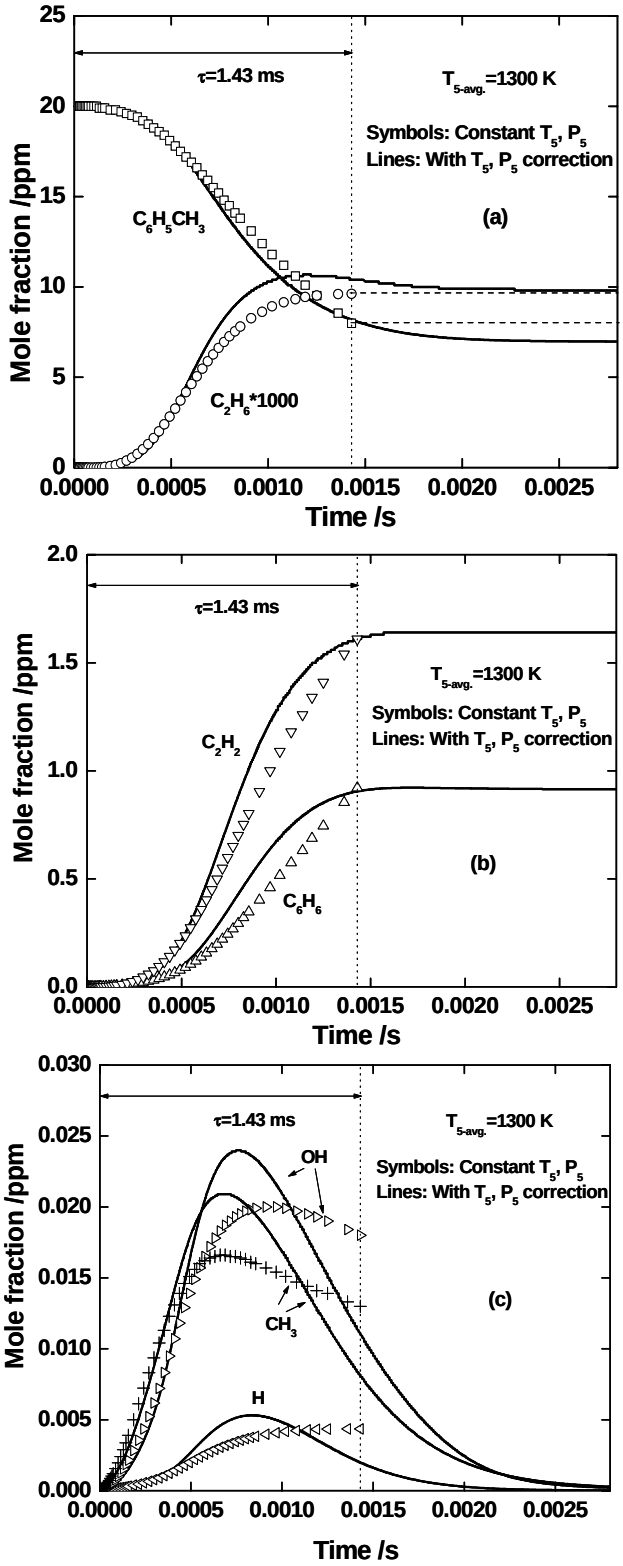

Fig 30: Time dependent P5 and T5 simulations. Predicted species mole fractions at nominal 600 bar using (1) constant and (2) time dependent T_5 and P_5. Simulation was performed using a toluene oxidation model (ref. 1) with a stoichiometric mixture of 0.002% C_7H_8–0.018% O_2–Ar. Panel (a): C_7H_8 and C_2H_6; panel (b): C_2H_2 and C_6H_6; panel (c): H, CH_3 and OH. Dashed lines in panel (a) were drawn for visualization of the deviations. See text for details.

for the consumption and production of these species.

The computational experiment with toluene oxidation suggests that there is only a minor effect of unaccounted for reactions during quenching on the modeling of stable species concentrations. To further probe whether or not this conclusion is unique to toluene oxidation, the same pressure and temperature profiles were utilized to simulate ethane oxidation using GRI-Mech 3.0[33] and a stoichiometric mixture of 0.02% C_2H_6–0.07% O_2–Ar. For this chemical system the overall errors were even less, probably due to the different mechanisms. We also extended the investigation to a pyrolysis experiment and again did not find significant differences. The relatively small impact of the reactions of radicals during quenching on stable species in both oxidizing and pyrolysis environments is plausible because of the relative low populations of the radical species compared to stable species and because of the multiple reaction routes of radicals that form multiple stable species since radical species generally participate in many barrierless or low barrier reactions.

It should also be emphasized that the "quality" of the pressure traces, the first hand experimental measurement indicating the degree of non-ideality behind reflected shock waves, is the key factor affecting the accuracy of kinetic simulation using constant T_5 and P_5 and empirical τ. There will be about a 8% temperature increase if the endwall pressure has a 20% increase, and in this case using average $T_{5\text{-avg}}$ will cause considerable deviations. Also if the pressure trace shows a long and slow cooling tail, kinetic contributions in the quenching period will be significant. Our computational experiments indicate that if pressure increases by less than 15% and then decreases to half its maximum value within 2.5 milliseconds, the overall error associated with conventional treatment in stable species predictions will be less than 10%. Fortunately, a "decent' , i.e. one with less than a 15% pressure rise and rapid decrease after the reaction period, shock profile can be easily achieved by tuning the shock tube configuration through taking advantage of the modular design of the UIC HPST[55]. When this is the case, kinetic simulations strictly according to conditions behind reflected shock waves may not be necessary with all its complications and the conventional treatment that considers constant T_5 and P_5 and ignores subsequent reactions during the quenching period is sufficient.

Recently in this laboratory a single detailed kinetic model for ethane oxidation and pyrolysis has been developed with shock tube data that were obtained over an extensive pressure range from 5-1000 bar[31]. The model, referred to as the modified Miller model, is based a series of work by Miller and co-workers[32]. The final model consists of 93 species and 535 reactions containing aromatic chemistry up to two rings. Our laboratory investigation has also found the model Gri-Mech 3.0[33], which was optimized against multiple data sets obtained primarily at pressures below 10 bar and contains 53 species and 325 reactions including the reactions of a number of C_2 and C_3 unsaturates, when used to predict ethane chemistry does not do a good job in predicting the measured species profiles. It is of great interest to choose these two models to examine the real gas impacts on the model development and validation against HPST data. In all our prior work on ethane oxidation and pyrolysis all kinetic simulations were performed using unaltered Chemkin programs, i.e. the ideal gas assumption was applied. To account for real gas impacts more species property data are required and necessary critical properties and acentric factors of all the species in the models were obtained in this work[67]. This

data was used with the Peng-Robinson (P-R) equation of state since, as Schmitt and Butler[72] demonstrated, the P-R equation compared with other types of EOS provided the most accurate correction for simulation of their observed detonation velocity at elevated pressures.

The computational experiments were first performed using a stoichiometric reagent mixture of 0.02% C_2H_6–0.07% O_2–Ar with an initial temperature of 1300 K at three different pressures: 100 bar, 613 bar and 1000 bar. The comparative results of C_2H_6 mole fraction predicted by the modified Miller and Gri-Mech 3.0 with and without real gas corrections are plotted in Figure 31. The other three measured species of C_2H_4, C_2H_2 and CO were also monitored but not graphically presented in this article. At 100 bar, the difference in the prediction using the ideal gas equation with the one using P-R equation is barely noticeable for all four species with C_2H_6 as an example shown in Figure 31(a). The deviation, however, is clear at 613 bar and even larger at 1000 bar, Figures 31(b) and 31(c) respectively. Generally real gas effects manifest themselves by reducing what might be called the induction time – the time to the start of observable fuel consumption. The higher the system pressure, the larger the shortening in induction time will be. Correspondingly, in the model a depleting species such as C_2H_6 is consumed faster and a growing species such as CO rises more quickly because of non-ideal gas effects. Similar phenomena were also observed with C_2H_4 and C_2H_2. Evidently, Figure 31 also indicates the different degree of real gas impacts on different kinetic models with the modified Miller model being slightly more sensitive.

From our results such as those shown in Figure 31, it would appear that at elevated pressures it is necessary to incorporate real gas effects in chemical kinetic simulations. However, this conclusion seemingly true for the time distribution of products at one temperature may not be true for many reaction products as a function of temperature – the way data are obtained from the shock tube. In order to examine the generality of real gas effects a comparative study was conducted to reveal the predictions of the modified Miller model with and without real gas corrections against HPST data obtained at nominal 340 bar. Figure 32 shows the results with C_2H_6 in panel (a), C_2H_4 in panel (b), C_2H_2 in panel (c) and CO in panel (d). Somewhat surprisingly given our previous results Figure 32 indicates that the real gas impacts on the kinetic modeling are far less important than we initially thought. While it is true that for one specific data point at one temperature, the model predictions corrected by Peng-Robinson equation might different from those predicted using the ideal gas equation, over the whole temperature range, the corrected and uncorrected model predictions follow exactly the same tends. The same phenomenon is also found when performing a similar computational experiment with HPST data obtained at a nominal pressure of 1000 bar. Such a finding is of great importance because it implies that real gas effects will not affect the performance of a kinetic model derived from HPST data and in future work it may not be necessary to incorporate real gas correction into kinetic modeling of experimental data obtained in a wide temperature range and the current practice of using Chemkin with the ideal gas assumption embedded in the calculations can continue. It appears, as perhaps would be expected, that the choice of reactions with their attendant rate parameters is the primary determinant of the ability of a model to simulate high pressure shock tube data.

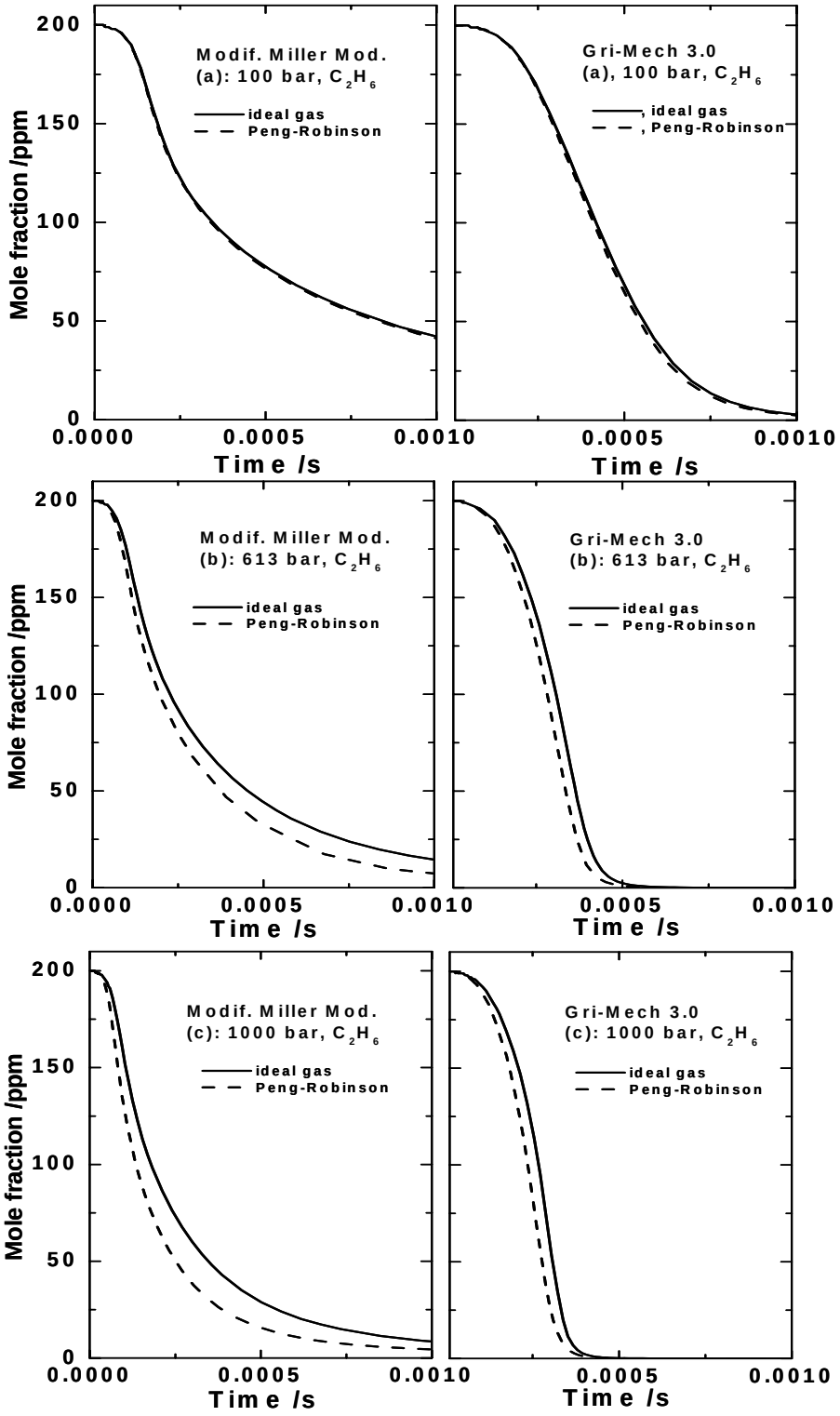

Fig 31: Real gas impacts on ethane profile at three different pressures of (a) 100 bar, (b) 613 bar and (c) 1000 bar. Solid lines: ideal gas equation used; dashed lines: real gas corrected by Peng-Robinson equations. Simulation was perform using two different kinetic models of (1) modified Miller (ref 54) and Gri-Mech 3.0 (ref 26) on a stoichiometric mixture of 0.02% C_2H_6–0.07% O_2–Ar at an initial temperature of T_0 = 1300 K.

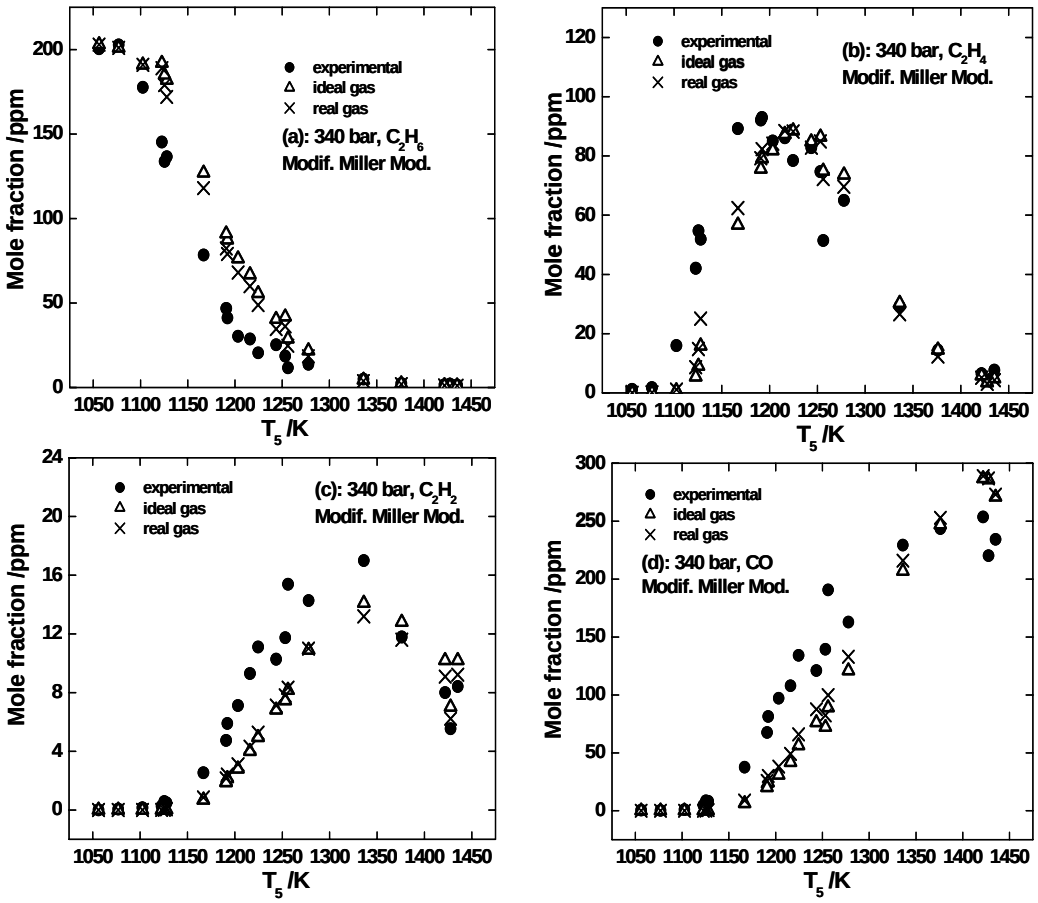

Fig 32: Real gas impacts on the development and validation of a detailed kinetic model against HPST data obtained at 340 bar over a wide temperature range. The reaction time ranged from 1.0 ms to 1.8 ms. Closed circles: experimental data; open triangles: predictions using ideal gas equation; crosses: predictions with real gas correction using Peng-Robinson equation. The modified Miller model (ref 54) was used. See text for detailed discussions.

(g) Diacetylene Pyrolysis:

Diacetylene despite being a known soot precursor is often overlooked in soot formation models because of limited experimental studies involving its formation/decomposition as well as lack of validated kinetic parameters under combustion conditions. In order to supplement the lack of detailed experimental studies as well as model its high temperature decomposition chemistry, we have initiated studies on diacetylene decomposition under practical combustion conditions[73].

C_4H_2, the reactant, is not available commercially nor are there any direct precursors that are available that would be a clean source for C_4H_2 under the conditions behind a shock wave. Consequently the first step involves a synthesis of C_4H_2. Diacetylene was synthesized[73] using 1,4 dichloro-2-butyne as the starting material using the synthetic route suggested by Prof. Henning Hopf[74]. This procedure is similar to the one suggested by Brandsma[75], but differed in the way the diacetylene was trapped as described now. 1,4 dichloro-2-butyne reacts with KOH in the presence of dimethylsulfoxide (DMSO) to form diacetylene and some acetone as by product. The diacetylene and acetone thus formed are swept by the Ar, which acts as a carrier gas as well as keeping the concentration in the system as low as possible. The majority of the

acetone is condensed back into the mixing flask by the condenser. The diacetylene is then sent to the traps for collection and removal of trace impurities. Collection of diacetylene was carried out in three separate cold traps as illustrated in Figure 33 which depicts the synthetic procedure. The first trap was kept at -10^{o}C where acetone was trapped. The second trap was maintained at -70^{o}C where diacetylene was collected along with other trace impurities which included unreacted reagents. The third trap was maintained at -170^{o}C where over 97% pure diacetylene was collected.

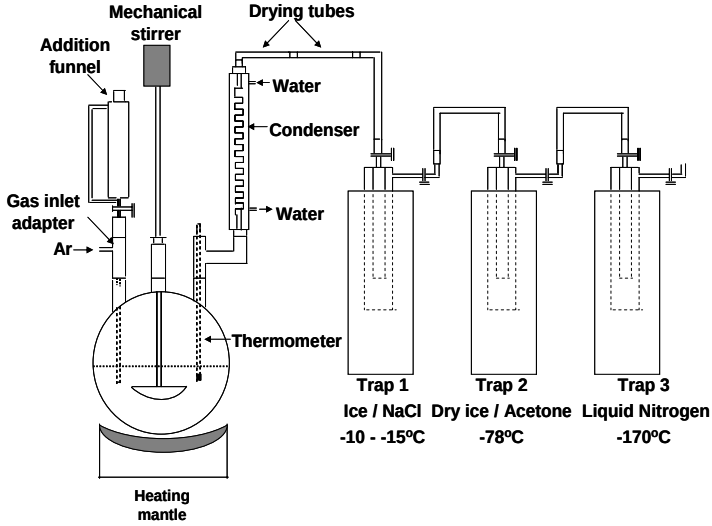

Fig 33: Schematic for diacetylene synthesis

Another difference in this method is in avoiding the use of tetrahydrofuran (THF) as a solvent for trapping diacetylene. Due to the absence of THF, the diacetylene mixtures were made easier. The purity of the synthesized diacetylene was estimated using GC/MS and was found to be 98%+. The synthesized C_4H_2 which was maintained at -170^{o}C in a cold trap was immediately admitted manometrically into a mixture tank and diluted using the bath gas Argon (99.999%, AIRGAS) to obtain desired initial mole fractions of C_4H_2 that range from 5-100 ppm. Neon (Research Grade, BOC Gases), the internal standard used to check for dilution effects was also admitted into the mixture tank.

Experiments were performed over a wide temperature range from 1100 K to 1800 K and at high pressures from 35-300 atm using the UIC high pressure single pulse shock tube[73]. Dilute reagent mixtures from 4-400 ppm were used in these experiments. The shock tube has been heated to 100^{0}C in order to permit condensable species such as the heavier polyacetylenes to be sampled. The primary intermediates observed in these experiments were C_2H_2, C_6H_2 and H_2 with trace amounts of allene, propyne, vinyl acetylene and benzene. In order to rule out the effects of small amounts of impurities that might play a role in catalyzing the reactions, we have performed experiments using mixtures with initial C_4H_2 mole fractions 20 ppm and 5 ppm. For example the 100 ppm mixture contains not more than 2 ppm impurities that drops down to the order of sub-ppm and ppb levels with the 20 and 5ppm mixture which are insignificant for all practical purposes. Consequently any effect of impurities is practically ruled out in these experiments.

Figure 34 depicts representative profiles for C_4H_2 decay from the 50 and 100 atm

data sets. The rate of decomposition of C_4H_2 is slower in the case of 50 atm experiments as compared with the 100 atm experiments an indication that the rate controlling steps are not at the high pressure limit.

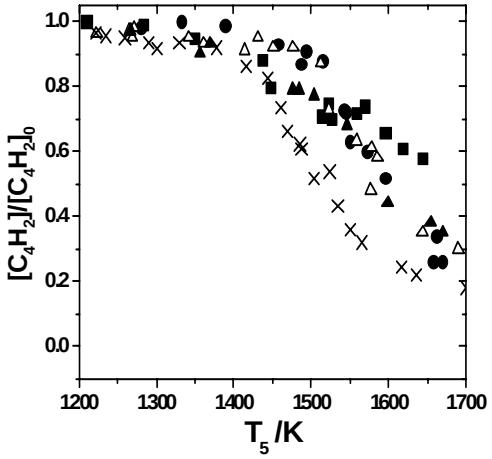

Fig 34: C_4H_2 decay. [■] 50 atm 5 ppm, [▲] 50 atm 20 ppm,[●] 50 atm 100 ppm, [Δ] 100 atm 5 ppm, [X] 100 atm 100 ppm

The experimental data has been simulated using two of the available literature models for diacetylene decomposition. Figure 35 shows the results of simulations using the Kiefer et al.[76] and the Hidaka et al.[11] models for the 100 atm, 100 ppm C_4H_2 pyrolysis experiments. Figure 35 shows that both the models fail to capture the experimental C_4H_2 decomposition profiles. While the Kiefer et al. model[76] predicts the onset of decomposition of C_4H_2 at temperatures above 1525 K, in the Hidaka et al.[11] model the decomposition of C_4H_2 does not occur below 1700 K. The reactions affecting the decomposition of C_4H_2 in either of these models appear to be primarily $C_2H+C_2H_2=C_4H_2+H$ and $C_4H_2+H=C_4H_3$.

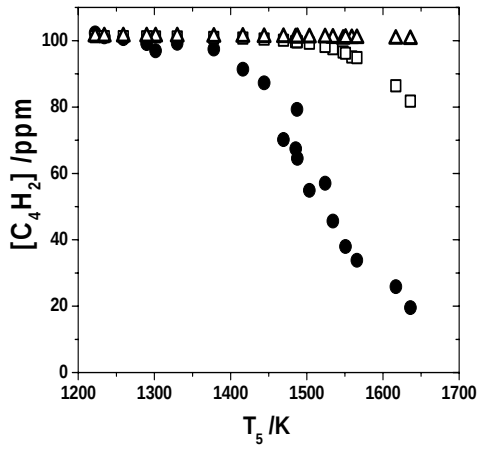

Fig 35: C_4H_2 Modeling. C_4H_2 pyrolysis, 100 atm 100 ppm. [●] Expt Data, [□] Kiefer et al., [Δ] Hidaka et al.

Despite the inability of the two current kinetic models to accurately predict the experimentally observed species profiles for the pyrolysis of C_4H_2 the Kiefer et al.[76] model because of its better predictive capability appears to be a better base model for further analysis. We have updated the thermochemistry as well as incorporated P dependent rate constants for key bimolecular steps in the Kiefer et al.[76] model which

show improved predictions in comparison to the experimental data. The simulations indicate the importance of fall-off considerations even at the high P at which this study was performed. Furthermore channels missing in current models involving the C_4H_3 isomers appear to be potentially important to describe the C_4H_2 decay and theoretical and modeling studies have been initiated to account for these reactions.

References

1. Sivaramakrishnan, R.; Tranter, R. S.; Brezinsky, K. *Proc. Combust. Inst.*, **2005** 30, 1165-1173.
2. Sivaramakrishnan, R.; Tranter, R. S.; Brezinsky, K. *Combust. and Flame*, **2004** 139, 340-350.
3. Klotz, S. D.; Brezinsky, K.; Glassman, I. *Proc. Combust. Inst.* **1998** 27, 337-344.
4. Dagaut, P.; Pengloan, G. ; Ristori, A. *Phys. Chem. Chem. Phys.* **2002** 4, 1846-1854.
5. Burcat, A.; Snyder, C; Brabbs, T. "Ignition Delay Times of Benzene and Toluene with Oxygen in Argon Mixtures", NASA TM 87312, **1986**.
6. Sivaramakrishnan, R.; Vasudevan, H.; Tranter, R. S.; Brezinsky, K. *Combust. Science and Tech.*, **2006** 178(1-3), 285-305.
7. Hou, K. C.; Palmer, H. B. *J. Phys. Chem.* **1965** 69, 863.
8. Laskin, A.; Lifshitz, A. *Proc. Combust. Inst.* **1996** 26, 669.
9. Banerjee, D. K.; Matei, V.; Vantu, V. *Rev. Roum. Chim.* **1982** 27, 621-628.
10. Wang, H.; Laskin, A.; Moriarty, N. W.; Frenklach, M. *Proc. Combust. Inst.* **2000**, 28, 1545.
11. Burcat, A. Third Millennium Ideal Gas and Condensed Phase Thermochemical Database for Combustion, TAE Report 867, **2001** Technion Aerospace Engineering Department, Israel.
12. Hidaka, Y.; Henmi, Y.; Ohonishi, T.; Okuno, T.; Koike, T. *Combust. and Flame* **2002** 130, 62-82.
13. Kern, R. D.; Chen, H.; Singh, H. J.; Xie, K.; Kiefer, J. H.; Sidhu, S. S. Turbulence and Molecular Processes in Combustion, *Proceedings of the Sixth Toyota Conference*, Ed. Takeno, T. Elsevier, The Netherlands, **1992**, 117-133.
14. Braun-Unkhoff, M.; Frank, P.; Just, TH. *Proc. Comb. Inst.* **1988** 22, 1053-1061.
15. Brouwer, L. D.; Muller-Markgraf W.; Troe, J. *J. Phys. Chem.* **1988** 92, 4905.
16. Hippler, H.; Reihs, C.; Troe, J. *Z. Phys. Chem. Neue Folge* **1990** 167, 1-16.
17. Sivaramakrishnan, R.; Tranter, R. S.; Brezinsky, K. *J. Phys. Chem. A*, **2006** 110, 9388-9399.
18. Bruinsma, O. L. S.; Geertsman, R. S.; Bank, P.; Moulijn, J. A. *Fuel* **1988** 67, 327-333.
19. Eng, R. A.; Gebert, A.; Goos, E.; Hippler, H.; Kachiani, C. *Phys. Chem. Chem. Phys.* **2002** 4, 3989-3996.
20. Baulch, D. L.; Bowman, C. T.; Cobos, C. J.; Cox, R. A.; Just, TH.; Kerr, J. A.; Pilling, M. J.; Stocker, D.; Troe, J.; Tsang, W.; Walker, R. W.; Warnatz, J. *J. Phys. Chem. Ref. Data* **2005**, 34(3), 757-1397.
21. Klippenstein, S. J.; Harding, L. B.; Georgievskii, Y. In Press, *Proc. Combust. Inst.* **2006.**

22. Ruscic, B.; Boggs, J. E.; Burcat, A.; Csaszar, A. G.; Demaison, J.; Janoschek, R.; Martin, J. M. L.; Morton, M.; Rossi, M. J.; Stanton, J. F. ; Szalay, P. G.; Westmoreland, P. R.; Zabel, F.; Berces, T. *J. Phys. Chem. Ref. Data* **2005**, 34(2), 573-656.
23. Burcat, A.; Ruscic, B. Ideal Gas Thermochemical Database with updates from Active Thermochemical Tables <ftp://ftp.technion.ac.il/pub/supported/aetdd/thermodynamics>;16 Sep 2005. mirrored at <http://garfield.chem.elte.hu/Burcat/burcat.html>; 16 Sep 2005.
24. Davico, G. E.; Bierbaum, V. M.; DePuy, C. H.; Ellison, G. B.; Squires, R. R. *J. Am. Chem. Soc.* **1995**, 117(9), 2590-2599.
25. Sivaramakrishnan, R.; Tranter, R. S.; Brezinsky, K. *J. Phys. Chem. A*, **2006** 110, 9400-9404.
26. Laskin A.; Lifshitz, A. *Proc. Combust. Inst.* **1998** 27, 313-320.
27. Oehlschlaeger, M. A.; Davidson, D. F.; Hanson, R. K. *J. Phys. Chem. A* **2006,** 110, 6649-6653.
28. Colket, M. B.; Seery, D. J. *Proc. Comb. Inst.* **1994** 25, 883-891.
29. Tranter, R. S.; Sivaramakrishnan, R.; Allendorf, M. D.; Brezinsky, K. Phys. Chem. Chem. Phys. **2002** 4, 2001-2010.
30. Tranter, R. S.; Raman, A.; Ramamoorthy, H.; Brezinsky, K.; Allendorf, M. D. *Proc. Combust. Inst.* **2002**, 29, 1267-1275.
31. Tranter, R. S.; Raman, A.; Sivaramakrishnan, R.; Brezinsky, K. *Int. J. Chem. Kin.* **2005** 37(5), 306-331.
32. Miller, J. A.; Klippenstein, S. J. *Proc. Combust. Inst.* **2000**, 28,1479.
33. Smith, G. P.; Golden, D. M.; Frenklach, M.; Moriarty, N. W.; Eiteneer, B.; Goldenberg, M; Bowman, C. T.; Hanson, R. K.; Song, S.;. Gardiner, W. C. Jr.; Lissianski, V. V.; Qin Z. http://www.me.berkeley.edu/gri_mech/
34. El Bakali, A. ; Dagaut, P. ; Pillier, L. ; Desgroux, P. ; Pauwels, J. -F.; Rida, A. ; Meunier, P. *Combust. and Flame* **2004** 137, 109-128.
35. Hidaka, Y.; Sato, K.; Hoshikawa, H. ; Nishimori, T.; Takahashi, R.; Tanaka, H.; Inami, K.; Ito, N. *Combust. and Flame* **2000** 120, 245-264.
36. Curtiss, L. A.; Raghavachari, K.; Trucks, G. W.; Pople, J. A. *J. Chem. Phys.* **1991** 94, 7221-7230.
37. Curtiss, L. A.; Raghavachari, K.; Redfern, P. C.; Rassolov, V.; Pople, J. A. *J Chem. Phys.* **1998** 109, 7764-7776.
38. Ochterski, J. W.; Petersson, G. A.; Montgomery, J. A. Jr.; *J. Chem. Phys.* **1996** 104, 2598-2619.
39. Sivaramakrishnan, R.; Tranter, R. S.; Brezinsky, K. *J. Phys. Chem. A*, **2005** 109, 1621-1628.
40. Frisch, M. J.; Trucks, G. W.; Schlegel, H. B.; Scuseria, G. E.; Robb, M. A.; Cheeseman, J. R.; Zakrzewski, V. G.; Montgomery, J. A. Jr.; Stratmann, R. E.; Burant, J. C.; Dapprich, S.; Millam, J. M.; Daniels, A. D.; Kudin, K. N.; Strain, M. C.; Farkas, O.; Tomasi, J.; Barone, V.; Cossi, M.; Cammi, R.; Mennucci, B.; Pomelli, C.; Adamo, C.; Clifford, S.; Ochterski, J.; Petersson, G. A.; Ayala, P. Y.; Cui, Q.; Morokuma, K.; Rega, N.; Salvador, P.; Dannenberg, J. J.; Malick, D. K.; Rabuck, D.; Raghavachari, K.; Foresman, J. B.; Cioslowski, J.; Ortiz, J. V.; Baboul, A. G.; Stefanov, B. B.; Liu, G.; Liashenko, A.; Piskorz, P.; Komaromi, I.;

Gomperts, R.; Martin, R. L.; Fox, D. J.; Keith, T.; Al-Laham, M. A.; Peng, C. Y.; Nanayakkara, A.; Challacombe, M.; Gill, P. M. W.; Johnson, B.; Chen, W.; Wong, M. W.; Andres, J. L.; Gonzalez, C.; Head-Gordon, M.; Replogle, E. S.; Pople, J. A. *Gaussian 98*, Revision A.11.3, Gaussian, Inc., Pittsburgh PA, **2002**.
41. *CS Chem3D Pro™ Version 3.5.1*, CambridgeSoft Corporation, **1997**.
42. Baboul, A. G.; Curtiss, L. A.; Redfern, P. C.; Raghavachari, K. *J. Chem. Phys.* **1999** 110, 7650-7657.
43. Notario, R.; Castano, O.; Abboud, J. –L. M.; Gomperts, R.; Frutos, L. M.; Palmeiro, R. *J. Org. Chem.* **1999** 64, 9011-9014.
44. Scott, A. P.; Radom, L. *J. Phys. Chem.* **1996** 100, 16502-16513.
45. Nicolaides, A.; Rauk, A.; Glukhovtsev M. N.; Radom, L. *J. Phys. Chem.* **1996** 100, 17460-17464.
46. Hehre, W.; Ditchfield, R.; Radom, L.; Pople, J. A. *J. Amer. Chem. Soc.* **1970** 92, 4796-4801.
47. Raghavachari, K.; Stefanov, B. B.; Curtiss, L. A. *J. Chem. Phys.* **1997** 106, 6764-6767.
48. Petersson, G. A.; Malick, D. K.; Wilson, W. G.; Ochterski, J. W.; Montgomery, J. A. Jr.; Frisch, M. J. *J. Chem. Phys.* **1998** 109, 10570-10579.
49. Wiberg, K. B. *J. Org. Chem.* **1997** 62, 5720-5727.
50. Afeefy, H. Y.; Liebman, J. F.; Stein, S. E. *Neutral Thermochemical Data in NIST Chemistry WebBook*, NIST Standard Reference Database Number 69**,** Eds. P.J. Linstrom and W.G. Mallard, **March 2003**, National Institute of Standards and Technology, Gaithersburg, MD, 20899 (http://webbook.nist.gov).
51. Sivaramakrishnan, R.; Tranter, R. S.; Brezinsky, K. "Accurate Thermochemistry using a New Ring Conserved Isodesmic Reaction Scheme-A DFT study of Aromatics and PAHs", Proceedings of the Fourth Joint Meeting of the U. S. Sections of the Combustion Institute, Paper A09, Philadelphia, March **2005**.
52. Yu, J.; Sumathi, R.; Green, W. H. *J. Amer. Chem. Soc* **2004** 126, 12685-12700.
53. Tsang, W. in *Shock Waves in Chemistry*. Lifshitz, A. (Ed.); Marcel Decker, New York, 1981, Ch.2.
54. Lifshitz, A. in *Handbook of Shock Waves*. Ben-Dor, G.; Igra, O.; Elperin, T. (Editors), Academic Press, San Diego, 2001, Vol. 3. *Chemical Reactions in Shock Waves and Detonations.*
55. Tranter, R. S.; Fulle D.; Brezinsky, K. *Rev. Sci. Inst.* **2001**, *72*, 3046.
56. Tranter, R. S.; Sivaramakrishnan, R.; Srinivasan, R.; Brezinsky, K. *Int. J. Chem. Kin*. **2001**, *33*, 722.
57. Hidaka, Y.; Shiba, S.; Takuma, H.; Suga, M. *Int. J. Chem. Kin*. **1985**, *17*, 441.
58. Peterson, E. L.; Hanson, R. K. *Shock Waves.* **2001**, *10*, 405.
59. Davidson, D. F.; Hanson, R. K. *Israel J. Chem.* **1996**, *36*, 321.
60. Michael, J. V.; Sutherland, J. W. *Int. J. Chem. Kin*. **1986**, *18*, 407.
61. Peterson, E. L., Davidson, D. F., Rohrig, M.; Hanson, R. K. *Intl. Symp. Shock Waves*. **1996**, *20*, 941.
62. Colket III, M. B. *Proc. Combust. Inst.* **1986**, *21*, 851.
63. Mackie, J. C.; Colket III, M. B.; Nelson, P. F. *J. Phys. Chem.* **1990**, *94*, 4099.
64. Gaydon, A. G.; Hurle, I. R. *The shock tube in High-Temperature Chemical Physics*. Reinhold Publishing Corp., New York, 1963.

65. Beattie, J. A. *Chemical Reviews.* **1949**, *44*, 141.
66. Schmitt R. G; Butler, P. B.; French, N. B. *Chemkin Real Gas*: A Fortran Package for Analysis of Thermodynamic properties and chemical kinetics in non-ideal systems, **1993**.
67. Tang, W.; Brezinsky, K. *Int. J. Chem. Kin.* **2006** 38(2), 75-97.
68. Kee, R. J.; Rupley, F. M.; Miller, J. A. "Chemkin-II: A Fortran Chemical Kinetics Package for the Analysis of Gas-Phase Chemical Kinetics" *Sandia National Laboratories Report SAND* 89-8009, **1990**.
69. Lutz, A. E.; Kee, R. J.; Miller, J. A. "SENKIN: A Fortran Program for Predicting Homogeneous Gas Phase Chemical Kinetics with Sensitivity Analysis" *Sandia National Laboratories Report* 87-8248, **1988**.
70. Tang, W. *Ph.D. thesis.* Department of Chemical Engineering, University of Illinois at Chicago, **2005**.
71. Lifshitz, A.; Suslensky, A.; Tamburu, C. *J. Phys. Chem. A.* **2003**, *107*, 4851.
72. Schmitt R. G; Butler, P. B. *Combust. Sci. Tech.* **1995**, *106*, 167.
73. Raman, A.; Sivaramakrishnan, R.; Brezinsky, K. Technical Meeting of the Central States Section of The Combustion Institute, GRC-NASA, Cleveland, **2006**.
74. Hopf, H. Personal communication.
75. Brandsma, L. Preparative Acetylenic Chemistry, 2nd Edition Elsevier Scientific Publishing Co, New York, 1988.
76. Kiefer, J. H.; Sidhu, S. S.; Kern, R. D.; Xie, K.; Chen, H.; Harding, L. B. *Combust. Sci. Tech.* **1992** 82, 101-130.

Refereed publications emanating from DOE support

1. Sivaramakrishnan, R.; Tranter, R. S.; Brezinsky, K. Proc. Combust. Inst., 2005 30, 1165-1173.
2. Sivaramakrishnan, R.; Tranter, R. S.; Brezinsky, K. Combust. and Flame, 2004 139, 340-350.
3. Sivaramakrishnan, R.; Tranter, R. S.; Brezinsky, K. J. Phys. Chem. A, 2006 110, 9388-9399.
4. Sivaramakrishnan, R.; Tranter, R. S.; Brezinsky, K. J. Phys. Chem. A, 2006 110, 9400-9404.
5. Tranter, R. S.; Sivaramakrishnan, R.; Allendorf, M. D.; Brezinsky, K. Phys. Chem. Chem. Phys. 2002 4, 2001-2010.
6. Tranter, R. S.; Raman, A.; Ramamoorthy, H.; Brezinsky, K.; Allendorf, M. D. Proc. Combust. Inst. 2002, 29, 1267-1275.
7. Tranter, R. S.; Raman, A.; Sivaramakrishnan, R.; Brezinsky, K. Int. J. Chem. Kin. 2005 37(5), 306-331.
8. Sivaramakrishnan, R.; Tranter, R. S.; Brezinsky, K. J. Phys. Chem. A, 2005 109, 1621-1628.
9. Tang, W.; Brezinsky, K. Int. J. Chem. Kin. 2006 38(2), 75-97.

Students graduated with DOE support

Raghu Sivaramakrishanan	Fall 00 – Fall 2002, MSE, Fall, 2004, PhD.
Ashwin Raman	Fall 00 – Spring 2005, MSE, 2007, PhD.
Weiyong Tang	Fall 01 – Spring 2005, PhD
Arun Satheesh Kumar Raju	Fall 01 – Fall 2004, MSE
Harikrishnan Vasudevan	Fall 01 – Fall 2004, MSE
Srinivas Durgam	Fall 01 – Spring 2005, MSE

Replies to reviewers comments for DOE contract renewal (April 2005)

In 2004 a proposal for renewal and continuation of the work initiated with DOE support was submitted to the U.S. Department of Energy, Office of Energy Research, Office of Basic Energy Sciences, Chemical Sciences Division. The renewal request was denied based on the reviewers' comments. At the time of receipt of the comments, we responded in detail to the comments despite termination of the program (except for a one year close out process). The following section includes all our responses to the reviewers as provided in April 2005 with some updates, as marked that have resulted from subsequent work.

Introduction

The UIC single pulse shock tube is probably the only active single pulse shock tube in the US currently and also the most vibrant group among the very few (2-3) single pulse groups in the world. The capability of the single pulse tube to obtain species profiles at high temperatures is unmatched by other conventional flow tube apparatus. Apart from this, the UIC single pulse tube is the only one capable of operating over a dynamic pressure range that spans close to 3 orders of magnitude (5-1000 bars) in the high pressure regime thereby enabling not only the study of reactions at their high pressure limit but also at conditions that exist in practical combustion (Diesel and HCCI engines operate at pressures up to 100 bars) devices. Furthermore a brief survey of single pulse shock tube work reveals that prior studies have involved only the pure pyrolysis of a variety of species in contrast to the studies in the UIC High Pressure Shock Tube in which the primary focus has been the oxidation chemistry with species profiles obtained over a wide temperature regime for the first time at high temperatures/pressures.

Reviewer 1 Comments

1. The reviewer pointed out that in several other laboratories the chemical thermometer reaction is carried out in-situ. However among the single pulse shock tube community at present only Dr. Wing Tsang (NIST) performs calibrations in-situ. However his work involves primarily unimolecular decompositions and consequently interference with the calibrant and its reactions (by choice of appropriate calibrants) are ruled out. Among the other single pulse tubes in operation Prof. Assa Lifshitz (Israel) uses chemical calibration externally similar to our

apparatus. His work parallels the work in the UIC tube in that he measures species profiles and builds detailed models based on these profiles. Consequently to avoid interference from the calibrant he uses the external calibration technique. No mention is made in the literature among other single pulse studies (Prof. John Mackie-Australia, Dr. Meredith Colket-UTRC) about the usage of calibrants. In general the other groups measure only shock velocities and by using ideal shock relations estimate the pressure and temperature behind the reflected shock wave. However it is a well recognized fact among the single pulse tube practitioners that even at low pressures (such as in Dr. Tsang's and Prof. Lifshitz's tubes)[1] chemical calibrants are to be used in order that non ideal flow dynamics behind the shock wave can also be accounted for. The validity and appropriateness of the external calibration technique are discussed in our chemical thermometer article[2].

2. The reviewer also points out wrongly that the calibration was performed in a very different regime. Calibrations are performed at the same pressures (conditions) at which we subsequently shock the molecule of interest. For details reviewer is directed to our recent publications and the chemical thermometer article[2].
3. The reviewer points out potential problems due to condensation on the walls as well as during expansion into a vessel. The walls and sample vessels are electropolished to reduce surface sites for condensation if it were relevant. For the ethane work condensation issues were not a problem. However even in this study dilute reagent mixtures were used (<300 ppm) and the data has been shown to be reliable and consistent[3-5]. For the work on the aromatic species (toluene and benzene) very dilute mixtures were used (no more that 85 ppm in toluene[6]) to avoid/overcome condensation issues. However to increase our capabilities heating systems have been installed for the shock tube as well as for the associated mixture and analytical setup which would allow us to actively pursue/further our aromatics oxidation program by studying the larger molecules outlined in the proposal.
4. Unfortunately the reviewer did not have access (during the time of the review) to the more recent publications which are now in print to assess better the quality of the experimental/modeling studies on toluene oxidation. The model development and validation is discussed in a recent publication[9]. The model has been tested against not only the single pulse tube data but also lower temperature flow reactor species profiles and shock tube ignition delay measurements thereby extending the validity of the model.
5. Since the time of the review a large part of the work has been published and consequently the reviewer's comment about the progress being modest is unjustified. Furthermore the reviewer mentioned that the published work is not innovative. However the experimental technique (single pulse at high pressures) is innovative and the only one of its kind. The data generated is unique and no parallel can be found. The use of the single pulse tube for oxidative (more complicated) work also represents an innovation (no prior single pulse tube studies on oxidation chemistry).
6. The reviewer's comments with regard to the lack of expertise in using/interpreting state of the art quantum chemical techniques are unjustified. Despite being primarily an experimental group, we use ab-initio techniques on a daily basis to interpret/analyze results. Apart from the routine use of currently available theoretical models we have also developed a new model for obtaining accurate thermochemistry

for aromatics/PAHs and their radicals which is an essential part of our aromatics program. The new technique (simple and cost effective) obtains comparable if not better results when compared against other state of the art techniques. The reviewer is referred to our recent article[10]. Currently work is in progress in obtaining energetics from potential energy surfaces, at a level comparable to work by other researchers reported in the literature, which are subsequently used to obtain reaction rates from theory. These rates will be used to model the single pulse shock tube data (Work in progress). UPDATE: Our thermochemistry work on PAH's, as described above is an example of our current routine use of quantum chemical theory to complement our experimental work. These types of calculations have now been used in our subsequent toluene pyrolysis work[7,8].

Reviewer 2 Comments

1. The reviewer's concerns with respect to the modeling/data are addressed in the published toluene oxidation articles[6, 9]. Also see point 4 in our response to reviewer 1's comments.
2. The reviewer has mentioned that the decomposition of phenyl is close to the high pressure limit at 13 bars[11]. However the extracted k_∞ for C_6H_5=o-C_6H_4+H from this high level computational study differs by an order of magnitude from work done by Wang et al.[12] subsequently using high level methods. There are no prior phenyl pyrolysis experiments in a single pulse tube. As mentioned in our proposal rates of biphenyl formation from phenyl pyrolysis as well as benzene formation from phenyl in the presence of an H atom source will aid in a better evaluation of the rates in the development of a model for describing phenyl pyrolysis. UPDATE: Our recently published study of benzene pyrolysis[13] has again emphasized the importance of determining the phenyl radical decomposition pathway and its kinetic parameters. Despite what the reviewer said, a definitive examination of phenyl radical decomposition is still to be conducted.
3. The reviewer has also questioned the need for studying benzyl decomposition. Mackie et al.[14] in their study were able to obtain only total rates for benzyl decay based on their benzyl decay profiles. They were also able to obtain a fit to their benzyl absorption profiles. In their quantum chemical study they have shown two pathways for the decomposition of benzyl to be feasible energetically. However there is no experimental verification of either pathway. The proposed benzyl experiments in the presence of an H atom source to trap radical intermediates can help clarify/validate the importance of the mechanistic routes suggested by Mackie. Furthermore species profiles from the proposed benzyl experiments and the subsequent modeling can be used to refine the benzyl decay sub-chemistry in our current toluene model. UPDATE: Our recent toluene pyrolysis experiments have again highlighted the importance of studying benzyl decomposition despite what the reviewer said. In the absence of detailed benzyl decomposition data we needed to resort to global modeling to reasonably simulate our shock tube data from toluene pyrolysis. One of the conclusions of our study was that direct examination of benzyl reactions is necessary[8].

4. The reviewer has mentioned that there are extensive studies on the aromatic systems of interest. However there is minimal data in the literature on the oxidation of aromatics[6,9]. The completed work on toluene oxidation represents the first high temperature (high pressure) oxidation study using a shock tube. Prior studies have been performed using flow reactors at lower temperatures/pressures. Apart from two flow reactor studies there are only ignition delay measurements for toluene oxidation. In the case of xylene the data are sparse with only one prior flow reactor study and no detailed model. The lack of data as well as detailed models for these key fuel components necessitates experiments using the UIC single pulse tube.
5. The reviewer has also mentioned a possible overlap between the DOE and existing NSF grants. The NSF work was primarily on soot precursor chemistry, with the focus being the study of the formation of the first aromatic ring (benzene). Experiments/detailed modeling involving 1, 5-hexadiyne pyrolysis and C_3H_3 recombination have been performed to validate mechanistic routes involved in the complex C_3H_3+C_3H_3 surface. In contrast to the NSF study in which the focus was the formation chemistry (pyrolysis) for the first ring, the DOE work is primarily concerned with the destruction (oxidation and pyrolysis) chemistry of the primary aromatics (benzene, toluene and xylene). UPDATE: Prior NSF work on soot precursor formation has successfully been completed and even though it did not overlap with the proposed work, any questions about it are now moot.
6. The reviewer also questioned the need for another GC. At present the only rate limiting step for performing experimental work is the analysis run times associated with performing well resolved chromatographic separations for a wide array of species that result from our single pulse experiments (Analyses have been performed for permanent gases, C1-C9 hydrocarbons/aromatics in prior work). Work on larger aromatics will involve more species. An additional standard GC, not "custom made" as the reviewer seems to think, would help to reduce analyses times by having dedicated GCs for separate sets of species.

Reviewer 3 Comments

1. The reviewer mentioned the absence of experimental traces and simulation results in the proposal. Substantial amounts of experimental traces/species profiles and modeling results (sensitivity analyses) can be found in our recent publications[2-6,9].
2. The reviewer also mentioned that experiments should be conducted at pressures that overlap other research groups. Our ethane study spans pressures from 5 bars-1000 bars. The lower end of pressure range spans the pressure range of experiments performed in other facilities. In the case of the toluene work (P=25-600 bars and 1200 K<T<1500 K) complementary modeling of flow reactor data (P=1 atm and T<1200 K) and shock tube ignition delays (P=2-8 atm and 1200 K<T<1800K) were also performed. The ethane model was also used to simulate data from other laboratories.
3. The reviewer suggested the use of optical measurements of temperatures. At present work is in progress to obtain measurements using a fast response thermocouple.

4. The time history of reaction conditions in the shock tube as well as its effect on modeling have been studied recently. This work has been submitted to the International Journal of Chemical Kinetics in March 2005 and is expected to be published soon. UPDATE: Our extensive study of reaction conditions in the shock and the validity of the kinetics data we obtain has been published. The study confirms all our operating assumptions and reaffirms the value of the high pressure single pulse shock tube as a device for chemical kinetic studies[15].

Reviewer 4 Comments

1. The reviewer has suggested that the use of the single pulse technique has resulted in the loss of valuable time dependent information. However there are a number of other investigators obtaining such time dependent information (Dr. J. V. Michael at Argonne, Dr. Peter Frank and his group-DLR Stuttgart and Prof. Hanson's group-Stanford) in shock tubes. In contrast to this, as mentioned earlier, the UIC high pressure single pulse tube is unique in the US. Time dependent information is however essential. Consequently we also model the data from time dependent experiments in combination with our data. In our recent toluene pyrolysis experiments[7,8] we have modeled H-atom time profiles from ARAS-Shock tube measurements of Braun-Unkhoff et al.[16] in combination with our high pressure single pulse species profiles.

Reviewer 5 Comments

1. The reviewer has suggested that the primary decomposition rates in toluene are well established. However prior studies by Kern et al.[17] have shown that the branching ratios are still not well established. UPDATE: Our recently published study of toluene pyrolysis[7] has led to a new evaluation of the primary decomposition rates and a new branching ratio. The reported results reveal just how uncertain the primary decomposition rates were and confirm our assertion, as proposed, that this study was very important. We conducted the study using the close out funding provided in our final year.
2. The reviewer has commented that the proposition to study benzyl decomposition is a very promising one. This is in contrast to reviewer 2 who suggested that further studies on benzyl decomposition were not required. UPDATE: As mentioned above, our published analysis of benzyl decomposition as deduced from toluene pyrolysis studies[8] indicate that direct studies of the decomposition are still warranted.
3. The concern about using halogen containing precursors for generation of radicals is unwarranted since in our experiments the precursor concentrations are very low and the halogens preferentially recombine.

Reviewer 6 Comments

1. The reviewer has commented that there was a lack of methods for estimating pressure/temperature dependence. However in our high pressure experiments we

have observed no evidence for fall off. Furthermore in other work performed in the laboratory we have demonstrated the ability to obtain k(T,P) from Master Equation analyses. We have demonstrated all the fundamental chemical analysis necessary as the chemical systems warrant it.

2. The reviewer has mentioned that one of the reactions suggested in the proposal is spin forbidden and that several reactions are unlikely/unjustified. We have adopted overall steps to represent multiple pathways such as $C_6H_5CH_2=C_5H_5+C_2H_2$. Benzyl decomposition is not sufficiently well characterized both experimentally and theoretically and consequently we have adopted such an overall reaction to explain our acetylene profiles which depend sensitively on the rate of this reaction. Furthermore since the reviewer did not have access to our recent publications[6-9] he could not judge the model development/reaction analysis capabilities. We are curious too about the important reaction paths that the reviewer claims are missing since he mentions none in particular.

References

1. Tsang W. in The Handbook of Shock Waves, Volume 3, Gabi Ben-Dor, Ozer Igra and Tov Elperin, Eds., Academic Press, San Diego, CA, 2001 and W. Tsang, Shock Waves in Chemistry, Ch. 2, A. Lifshitz (Ed.), Marcel Dekker, New York, 1981.
2. Tranter, R.S., Sivaramakrishnan, R., Srinivasan, N. K. and Brezinsky K., International Journal of Chemical Kinetics, 33,722-731, 2001.
3. Tranter, R. S., Sivaramakrishnan, R., Allendorf, M. D. and Brezinsky, K., Physical Chemistry Chemical Physics, 4, 2001-2010, 2002.
4. Tranter R.S., Ramamoorthy H., Raman A., Brezinsky K., Allendorf M.D., Proc. Combust. Inst., 29, 1267-1275, 2002.
5. Tranter R. S., Raman A., Sivaramakrishnan R., Brezinsky K., Int. J. Chem. Kin., 37, 306-331, 2005.
6. Sivaramakrishnan R., Tranter R. S., Brezinsky K., Combustion and Flame, 139,340-350, 2004.
7. Sivaramakrishnan R., Tranter R. S., Brezinsky K., J. Phys. Chem. A, 110(30), 9388-9399, 2006.
8. Sivaramakrishnan R., Tranter R. S., Brezinsky K., J. Phys. Chem. A, 110(30), 9400-9404, 2006.
9. Sivaramakrishnan R., Tranter R. S., Brezinsky K., Proc. Combust. Inst., 30, 1165-1173, 2005.
10. Sivaramakrishnan R., Tranter R. S., Brezinsky K. J. Phys. Chem. A, 109, 1621-1628, 2005.
11. Madden, L. K.; Moskaleva, L. V.; Kristyan, S.; Lin, M. C., J. Phys. Chem. A, 101, 6790-6797, 1997.
12. Wang H., Laskin A., Moriarty N. W., Frenklach M., Proc. Comb. Inst., 28, 1545-1555, 2000
13. Sivaramakrishnan R., Vasudevan H., Tranter R.S., and Brezinsky K., Comb. Sci. Tech., 178 (1-3), 285-305, 2006.
14. Jones J., Backsay G. B., Mackie J. C., J. Phys. Chem. A, 101, 7105-7113, 1997.
15. Tang, W.; Brezinsky, K. Int. J. Chem. Kin. **2006** 38(2), 75-97.

16. Braun-Unkhoff, M.; Frank, P.; Just, TH. Proc. Combust. Inst., 22, 1053-1061, 1988.
17. Kern R. D., Chen H., Singh H. J., Xie K., Kiefer J. H. and Sidhu S. S., Thermal Dissociation Studies of Toluene at High Temperatures, Turbulent and Molecular Processes in Combustion, Proceedings of the Sixth Toyota Conference, Japan, Ed. T. Takeno, Elsevier, The Netherlands, 1992.